Journal of Contaminant Hydrology xxx (2014) xxx–xxx

Contents lists available at ScienceDirect

Journal of Contaminant Hydrology

journal homepage: www.elsevier.com/locate/jconhyd

Groundwater salinity in a floodplain forest impacted by saltwater intrusion

David A. Kaplan [a,*], Rafael Muñoz-Carpena [b]

[a] Department of Environmental Engineering Sciences, University of Florida, PO Box 116350, Gainesville, FL 32611, USA
[b] Department of Agricultural and Biological Engineering, University of Florida, PO Box 110570, Gainesville, FL 32611, USA

ARTICLE INFO

Article history:
Received 15 November 2013
Received in revised form 5 April 2014
Accepted 22 April 2014
Available online xxxx

Keywords:
Saltwater intrusion
Floodplain forest
Coastal wetlands
Bald cypress
Groundwater modeling
Salinity
Wetland restoration
River restoration
Time series analysis

ABSTRACT

Coastal wetlands occupy a delicate position at the intersection of fresh and saline waters. Changing climate and watershed hydrology can lead to saltwater intrusion into historically freshwater systems, causing plant mortality and loss of freshwater habitat. Understanding the hydrological functioning of tidally influenced floodplain forests is essential for advancing ecosystem protection and restoration goals, however finding direct relationships between hydrological inputs and floodplain hydrology is complicated by interactions between surface water, groundwater, and atmospheric fluxes in variably saturated soils with heterogeneous vegetation and topography. Thus, an alternative method for identifying common trends and causal factors is required. Dynamic factor analysis (DFA), a time series dimension reduction technique, models temporal variation in observed data as linear combinations of common trends, which represent unexplained common variability, and explanatory variables. DFA was applied to model shallow groundwater salinity in the forested floodplain wetlands of the Loxahatchee River (Florida, USA), where altered watershed hydrology has led to changing hydroperiod and salinity regimes and undesired vegetative changes. Long-term, high-resolution groundwater salinity datasets revealed dynamics over seasonal and yearly time periods as well as over tidal cycles and storm events. DFA identified shared trends among salinity time series and a full dynamic factor model simulated observed series well (overall coefficient of efficiency, $C_{eff} = 0.85$; $0.52 \leq C_{eff} \leq 0.99$). A reduced multilinear model based solely on explanatory variables identified in the DFA had fair to good results ($C_{eff} = 0.58$; $0.38 \leq C_{eff} \leq 0.75$) and may be used to assess the effects of restoration and management scenarios on shallow groundwater salinity in the Loxahatchee River floodplain.

1. Introduction

Saltwater intrusion is the invasion of fresh or brackish surface water or groundwater by water with higher salinity (USGS, 2001) and has both natural (e.g., Flynn et al., 1995) and anthropogenic (e.g., Bechtol and Laurian, 2005) drivers. Saltwater intrusion can lead to rapid and catastrophic loss of coastal wetlands (Wanless, 1989), especially where several drivers act simultaneously (e.g., deep-water canals, which increase the inland extent of saltwater inflow, combined with accelerated sea-level rise, hurricanes, or severe drought) (McCarthy et al., 2001). While sea level has cycled up and down over the millennia, the coastal ecosystems currently ringing the continents have developed over a fairly stable period of sea-level rise (Wanless et al., 1994). Relatively fast-acting natural and anthropogenic drivers are currently

Abbreviations: DFA, dynamic factor analysis; DFM, dynamic factor model; GWEC, groundwater electrical conductivity; SWEC, surface water electrical conductivity; WTE, water table elevation; SWE, surface water elevation; R_{net}, net recharge; RK, river kilometer; C_{eff}, Nash and Sutcliffe coefficient of efficiency; AIC, Akaike's information criterion; POR, period of record.

* Corresponding author. Tel.: +1 352 392 8439.
E-mail address: dkaplan@ufl.edu (D.A. Kaplan).

http://dx.doi.org/10.1016/j.jconhyd.2014.04.005
0169-7722/

overwhelming coastal wetlands with more frequent, longer, deeper, and saltier inundation in many areas (Burkett et al., 2001). Saltwater intrusion in coastal wetlands causes plant stress or mortality from prolonged submergence and/or high salinities; erosion of wetland substrate; conversion of freshwater habitats to brackish or saltwater habitats; and the transition of coastal saltwater habitats to open water (DeLaune et al., 1994). Barlow (2003) provides a thorough review of the causes and impacts of saltwater intrusion on the US Atlantic Coast.

In systems where the causes of saltwater intrusion are primarily anthropogenic, the development of watershed and river management and restoration plans may allow ecological impacts to be minimized or reversed, and a robust understanding of hydrological dynamics is vital to assess the potential impacts of these efforts. However, the dynamics of saltwater intrusion are controlled by the interactive effects of tidal activity, the timing and volume of freshwater discharge, wind speed and direction, and density gradients caused by salinity. With diurnal tidal cycles, stochastic annual weather patterns, and decadal climate cycles, the dynamic behavior of saltwater intrusion is highly complex (Werner et al., 2013). Interactions between surface water, groundwater, and porewater in variably saturated matrices with heterogeneous soils, vegetation, and topography (e.g., Gardner et al., 2002; Kaplan et al., 2010a; Langevin et al., 2005) often make finding direct relationships between basic hydrological inputs difficult. For example, the frequency and duration of groundwater salinity exceeding a critical ecological threshold (Jassby et al., 1995) are functions of surface water elevation and salinity, tidal range, distance from the ocean, distance from the river channel, local elevation (microtopography), volume of fresh surface water flow, and the direction, volume, and salinity of groundwater fluxes (Liu et al., 2001; Melloul and Goldenberg, 1997; Wang, 1988), as well as soil hydraulic characteristics and vegetation properties.

Full-scale, density-dependent, numerical models of water table elevation and groundwater salinity such as SEAWAT (Guo and Langevin, 2002) and MOCDENS3D (Essink, 2001) can be useful for improving our understanding of physical systems (Langevin et al., 2005) and for assessing the potential effects of proposed management scenarios (Nassar et al., 2007), but require extensive subsurface stratigraphy and hydrogeology data to populate the model domain and often rely on simplifying assumptions to estimate model boundary conditions (Motz and Sedighi, 2009) and initial conditions (Lin et al., 2008). These models also focus almost exclusively on deeper groundwater systems, and may not be as useful for describing shallow groundwater, which can be in direct contact with coastal wetlands directly vía the root zone (Skalbeck et al., 2008) or through upward or lateral seepage (e.g., Gardner et al., 2002; Moffett et al., 2008). On the other hand, collection of long-term, high-resolution shallow water table elevation and salinity data can describe the dynamics (i.e., magnitude, range, daily, seasonal and interannual variation, etc.) and spatial variation of these variables (e.g., Lyons et al., 2007). However, using visual inspection and comparative statistics to develop relationships between multivariate time series can be difficult, subjective, and may not improve our understanding of the hydrological relationships that characterize the system (Ritter et al., 2007). Thus, an alternative method for sifting through complex datasets to identify possible shared trends and relationships is required.

In this study, we applied dynamic factor analysis (DFA), a multivariate times series dimension reduction technique, to investigate the complex groundwater salinity dynamics observed in the floodplain wetlands of the Loxahatchee River, a managed coastal river in southeastern Florida (USA). DFA is a statistical model, such that dynamic factor models (DFMs) produced by DFA are driven by measured data. Thus, the approach requires no a priori information about the physical system being modeled. The ability to model time series as a combination of common trends (representing unexplained variability) and explanatory variables is especially useful for analyzing complex environmental systems, where DFA can help assess what explanatory variables (if any) affect the time series of interest, and thus may be worthy of closer attention. DFA was initially developed to analyze variation in economic time series (Geweke, 1977) and was later adapted to include explanatory variables to improve understanding of variation in a variety of hydrological and ecological systems, including studies of: groundwater level and quality (Kaplan et al., 2010b; Kovács et al., 2004; Kuo and Chang, 2010; Márkus et al., 1999; Muñoz-Carpena et al., 2005; Ritter and Muñoz-Carpena, 2006; Ritter et al., 2007); soil moisture dynamics (Kaplan and Muñoz-Carpena, 2011; Ritter et al., 2009); commercial fisheries (Addis et al., 2008; Erzini, 2005; Tulp et al., 2008; Zuur and Pierce, 2004); maximum precipitation trends (Kuo et al., 2011); and most recently large-scale vegetation change (Campo-Bescos et al., 2013).

In this study, DFA was applied to study the interactions between floodplain groundwater salinity and other hydrological variables in the floodplain wetlands of the Loxahatchee River (Florida, USA), where watershed modifications and management have reduced freshwater flow and led to saltwater intrusion into historically freshwater ecosystems. This changing hydrology has been associated with a transition to salt-tolerant, mangrove-dominated communities as salt water advanced upstream (South Florida Water Management District [SFWMD], 2006). While intensive data collection and modeling efforts have been directed at developing appropriate surface water management and restoration goals (SFWMD, 2002, 2006), groundwater salinity has been largely overlooked. Thus, the specific objectives of this research are to: 1) investigate shallow groundwater salinity in the floodplain of the Loxahatchee River along several transects perpendicular to the river (from upriver, freshwater areas through downriver, tidal areas) and 2) apply DFA to investigate interactions between the groundwater salinity time series and other hydrological variables to identify (a) important common trends among the series and (b) external hydrological factors that most fully explain observed variation in the time series.

2. Materials and methods

2.1. Study site and experimental setup

The Loxahatchee River is located on the southeastern coast of Florida, USA (26° 59′ N, 80° 9′ W; Fig. 1) and was

Please cite this article as: Kaplan, D.A., Muñoz-Carpena, R., Groundwater salinity in a floodplain forest impacted by saltwater intrusion, J. Contam. Hydrol. (2014), http://dx.doi.org/10.1016/j.jconhyd.2014.04.005

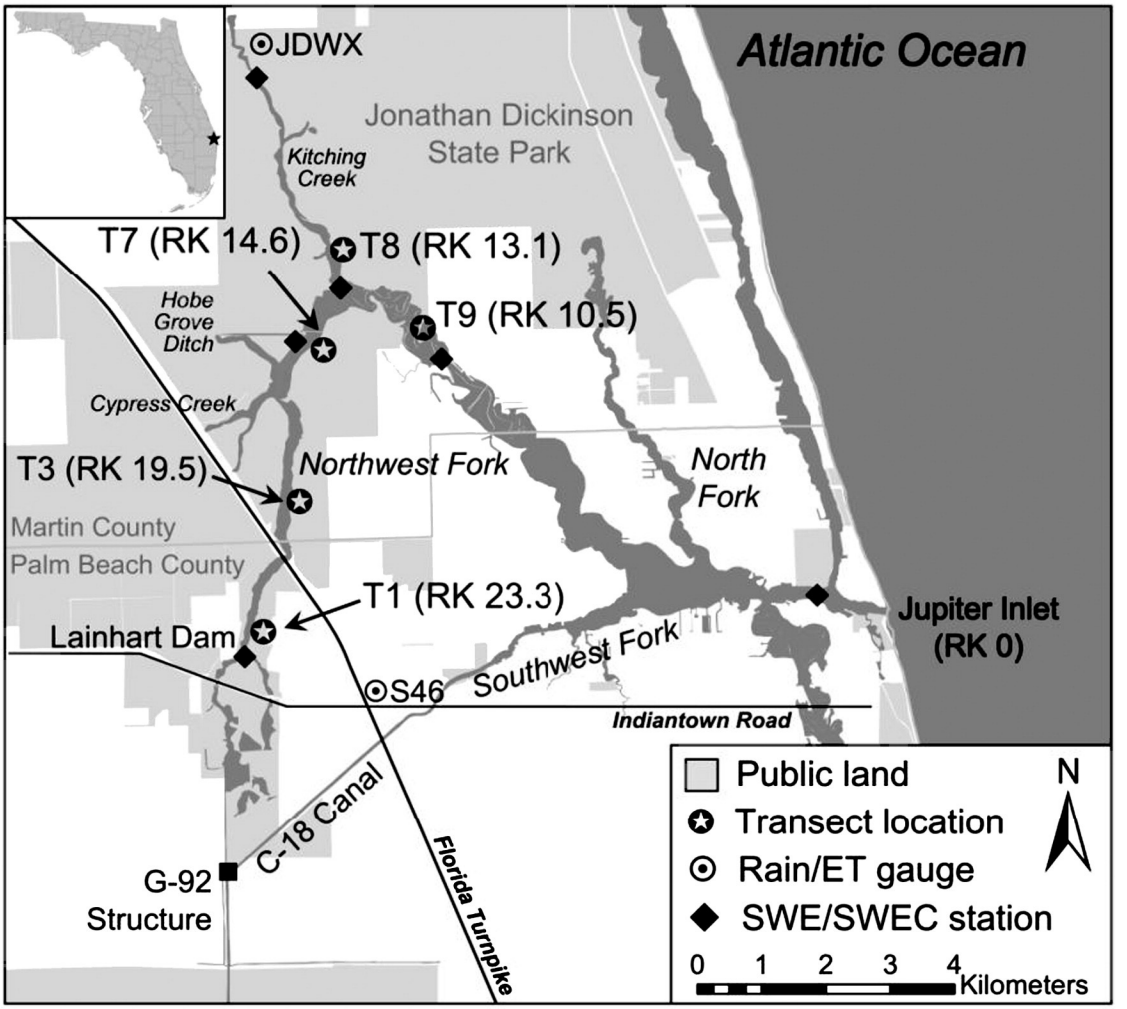

Fig. 1. The Loxahatchee River and surrounding area with transect locations (T1, T3, T7, T8, and T9), meteorological and surface water elevation (SWE) and electrical conductivity (SWEC) measurement locations, and major hydraulic infrastructure. Transect notation is followed by distance from river mouth (river kilometer, RK).

historically part of the greater Everglades watershed. The watershed drains approximately 550 km^2 in Palm Beach and Martin Counties and includes several large, publicly owned areas. The river's three main branches (the North, Southwest, and Northwest Forks) join in a central embayment that connects to the Atlantic Ocean via Jupiter Inlet (Fig. 1). The Loxahatchee River is often referred to as the "last free-flowing river in southeast Florida" (SFWMD, 2006) and in 1985, a 15.3-km stretch of the Northwest Fork (NW Fork) became Florida's first National Wild and Scenic River.

Altered hydroperiods and encroaching salinity in the NW Fork have been linked to undesired changes in the vegetative composition of the floodplain, where studies have documented the upriver retreat of bald cypress since at least the turn of the 20th century (Roberts et al., 2008). Of primary concern is the transition from bald cypress floodplain swamp to mangrove-dominated communities in the tidal floodplain as salinity increased and inadequate hydroperiod in the upstream riverine floodplain, which has shifted the system towards drier plant communities (SFWMD, 2009). Data collection and modeling efforts in the region have been underway for several years (e.g., Kaplan and Muñoz-Carpena, 2011; Kaplan et al., 2010a,b; Mortl et al., 2011; SFWMD, 2002, 2006, 2009; VanArman et al., 2005). Further description of the hydrological and ecological history of the NW Fork can be found in SFWMD (2006, 2009).

For this study, a network of twelve groundwater wells was developed along five vegetation survey transects (T1, T3, T7, T8, and T9; Fig. 1), encompassing a gradient of floodplain conditions that change with distance from the river mouth (indicated as river kilometer, RK). Water table elevation (WTE) and groundwater electrical conductivity (GWEC, expressed as specific conductance, S/m) data were collected every 30 min using TROLL 9000/9500 multi-parameter water quality probes (In-Situ Inc., Ft. Collins, CO, USA) from September 2004 through January 2009. To confirm probe readings, depth to the water table was measured using an interface meter (Solinst, Ontario, CA) and electrical conductivity (EC) probes were calibrated during each data download. Table 1 summarizes attributes of the twelve wells. A full

Please cite this article as: Kaplan, D.A., Muñoz-Carpena, R., Groundwater salinity in a floodplain forest impacted by saltwater intrusion, J. Contam. Hydrol. (2014), http://dx.doi.org/10.1016/j.jconhyd.2014.04.005

Table 1
Locations and attributes of the twelve groundwater wells in the study. Wells are distributed across five transects (T1, T3, T7, T8, and T9). River kilometer indicates distance from the river mouth. Well elevation denotes elevation at the ground surface.

Well	Transect type	River kilometer	Distance to river (m)	Well elevation (m, NGVD29)	Slotted elevation (m, NGVD29)
T1-W1	Riverine	23.3	50	3.28	1.51 to 2.12
T3-W1	Riverine	19.5	95	1.60	−0.16 to 1.36
T7-W1	Transitional	14.6	2	0.36	−1.49 to −0.88
T7-W2			30	0.43	−1.40 to −0.79
T7-W3			90	0.56	−1.13 to −0.52
T7-W4			130	2.94	−0.73 to 0.79
T8-W1	Upper tidal	13.1	5	0.12	−1.50 to −0.89
T8-W2			65	0.36	−1.24 to −0.63
T8-W3			105	2.28	−0.36 to 1.16
T9-W1	Lower tidal	10.5	70[a]	0.41	−1.45 to −0.84
T9-W2			50[a]	0.62	−1.24 to 0.28
T9-W3			30[a]	2.94	−1.31 to 0.22

[a] Shortest distance from well to river (T9 is on a peninsula).

description of the groundwater dataset and QA/QC procedure can be found in Muñoz-Carpena et al. (2008) and an in-depth analysis of WTE data is available in Kaplan et al. (2010b).

2.2. Dynamic factor analysis

DFA is a multivariate application of classic time series analysis and models temporal variation in observed data series as linear combinations of one or more non-linear common trends (representing unexplained variability), zero or more non-linear external explanatory variables (representing explained variability), a constant intercept parameter, and noise (Zuur et al., 2003); thus DFMs are linear combinations of non-linear factors. DFA is capable of modeling relatively short, incomplete, non-stationary time series (Zuur et al., 2003) and aims to balance goodness-of-fit and model parsimony; we assessed DFM performance using the Nash and Sutcliffe coefficient of efficiency ($-\infty \le C_{eff} \le 1$; Nash and Sutcliffe, 1970) and Akaike's information criterion, AIC (Akaike, 1974).

As opposed to physically based models, which are built upon the mechanisms known to underlie a given system, DFMs are built upon the common patterns among, and interactions between, response variables and explanatory factors. Thus, no a priori understanding of the interactions between response and explanatory time series is required (Ritter et al., 2009). DFA identifies one or more common trends among the response time series that represent unexplained, but shared, variation. The best DFM minimizes the number of common trends required to achieve a good fit as determined by C_{eff} and/or AIC. Appropriate explanatory variables may help improve the model and point out which environmental factors (if any) affect the response variables.

DFA endeavors to model a set of N time series (dubbed response variables) using M common trends ($M < N$), K explanatory variables, a level or intercept parameter, and noise (Lütkepohl, 1991; Zuur et al., 2003):

$$S_n(t) = \sum_{m=1}^{M} \gamma_{m,n}\alpha_m(t) + \mu_n + \sum_{k=1}^{K} \beta_{k,n}v_k(t) + \varepsilon_n(t) \quad (1)$$

$$\alpha_m(t) = \alpha_m(t-1) + \eta_m(t) \quad (2)$$

where $s_n(t)$ is a vector containing the set of N response variables; $\alpha_m(t)$ is a vector containing the mth common trend; $\gamma_{m,n}$ are factor loadings or weighting coefficients, which indicate the importance of each of the common trends within the DFM; μ_n is a constant level parameter; $v_k(t)$ is a vector containing 0–K explanatory variables; and $\beta_{k,n}$ are regression parameters, which indicate the importance of each of the explanatory variables in the DFM. In this study, N represents the twelve GWEC time series. $\varepsilon_n(t)$ and $\eta_m(t)$ are independent, Gaussian noise with zero mean and unknown covariance matrix. Common trends are predicted using the Kalman filter/smoothing algorithm and Expectation Maximization (EM) technique (Dempster et al., 1977; Shumway and Stoffer, 1982; Wu et al., 1996) and are modeled as a random walk (Harvey, 1989). The EM technique is also used to calculate factor loadings ($\gamma_{m,n}$) and level parameters (μ_n). Regression parameters ($\beta_{k,n}$) are modeled using linear regression (Zuur and Pierce, 2004).

The relative importance of common trends and explanatory variables was quantified using their associated factor loadings ($\gamma_{m,n}$) and regression parameters ($\beta_{k,n}$). The significance of relationships between response and explanatory variables was determined using the magnitude of the $\beta_{k,n}$ and their associated standard errors to calculate a t-value for each (significant for t-values > 2). Canonical correlation coefficients ($\rho_{m,n}$) were used to quantify cross-correlation between response variables and common trends, with values of $\rho_{m,n}$ close to unity indicating high correlation between a common trend and response variable. In the following sections, "minor" correlations refer to those with $|\rho_{m,n}| < 0.25$; "low" correlations to $0.25 \le |\rho_{m,n}| < 0.50$; "moderate" correlations to $0.50 \le |\rho_{m,n}| \le 0.75$; and "high" correlations to $|\rho_{m,n}| > 0.75$.

2.3. Explanatory variables

Meteorological and hydrological variables were used as candidate explanatory variables in the DFA. A total of 45 time series (each with 1588 daily average values) were investigated for use as possible explanatory variables in the DFA (Table 2). Since multi-collinearity may exist between explanatory variables measured at nearby locations, not all candidate explanatory variables were used in final DFMs. The variance inflation factor (VIF) was used to quantify the severity of multi-collinearity of each set of explanatory

Please cite this article as: Kaplan, D.A., Muñoz-Carpena, R., Groundwater salinity in a floodplain forest impacted by saltwater intrusion, J. Contam. Hydrol. (2014), http://dx.doi.org/10.1016/j.jconhyd.2014.04.005

Table 2
Hydrological time series used in the DFA.

Variable	Series type	No. of series	Description
GWEC	Response	12	Groundwater electrical conductivity (S/m) from wells in the Loxahatchee River floodplain
R_{net}	Explanatory	2	Cumulative net recharge (cumulative rainfall − cumulative ET_o, mm) calculated from the S-46 and JDWX weather stations
SWE	Explanatory	6	Surface water elevation (m, NGVD29) from stations in the NW Fork at RK 23.3 (near T1), RK 14.6 (near T7), RK 13.1 (near T8), RK 9.5 (near T9), RK 1.1 (near Jupiter Inlet), and on Kitching Creek
SWEC	Explanatory	8	Surface and/or bottom surface water electrical conductivity (S/m) from stations in the NW Fork at RK 24.0, RK 14.6, RK 13.1, RK 9.5, and RK 1.1
WTE/WTE_R	Explanatory	14	Water Table Elevation (WTE, m, NGVD29) from the twelve wells in this study and two single WTE trends—one calculated from the five highest-elevation wells in this study (WTE) and one calculated from nine regional USGS wells in and around the Loxahatchee River watershed (WTE_R)
CFD	Explanatory	7	Calculated cumulative flow deficit (km^3) based on flow at Lainhart Dam (RK 23.3) (see explanation in text)
CSS	Explanatory	8	Calculated cumulative salinity deviation (S/m) from SWEC stations (see explanation in text)

variables (Zuur et al., 2007), and combinations of explanatory variables with VIFs > 5 were not used in these analyses (Ritter et al., 2009).

Breakpoint rainfall data were acquired from two locations: the S-46 structure and in Jonathan Dickinson State Park, where daily reference evapotranspiration (ET_0) values were also measured (JDWX weather station Fig. 1). These data are available through the SFWMD's online database DBHYDRO (Stations S46_R and JDWX; www.sfwmd.gov/dbhydro/). Since GWEC data are autocorrelated (i.e., GWEC at time t is dependent on GWEC at $t - 1$), while this is not true for rainfall and ET, the difference between cumulative rainfall and cumulative ET_o was used to calculate two net recharge (R_{net}) time series to make this data potentially useful in the DFA (Ritter et al., 2009). Rainfall collected at the two stations had low correlation ($r^2 = 0.18$) and considerably different cumulative rainfall totals over the four-year study period. The effect of this spatial variability on model results was explored by developing DFMs using each of the R_{net} series, both series, and their average and comparing model results.

Surface water elevation (SWE) and surface water EC (SWEC) data were recorded at five stations in the NW Fork and one station upstream on Kitching Creek (Fig. 1). A SFWMD monitoring station on the headwater side of Lainhart Dam (0.45 km upstream of T1) measured average daily SWE and is available on DBHYDRO (station LNHRT_H). The Loxahatchee River District (LRD) maintains a water quality monitoring station (datasonde station 69) on the Northwest Fork at Indiantown Road that measured SWEC hourly (data acquired from LRD staff). United States Geological Survey (USGS) monitoring stations located at RK 14.6 (adjacent to T7), RK 13.1 (at confluence with Kitching Creek, near T8), RK 9.5 (~0.8 km downstream of T9), RK 1.1 (near the Jupiter inlet), and 2.8 km upstream of the confluence of the NW Fork with Kitching Creek measured SWE and SWEC every 15 min (data acquired from USGS staff).

Daily average WTE from nine USGS wells in and around the Loxahatchee River watershed (denoted as WTE_R) are publicly available and were downloaded from the USGS National Water Information System (accessed at http://waterdata.usgs.gov/nwis/). Fitting one common trend to these nine series did a good job of representing WTE_R variation ($C_{eff} = 0.83$) and was used as a (single) potential explanatory variable in this analysis.

Visual inspection suggested that variation in response variable (GWEC) time series might occur in a delayed and extended manner compared with candidate explanatory variables. To identify possible environmental variables that may better represent the dynamics of GWEC in the floodplain of the Loxahatchee River (and thus reduce the reliance of the final DFM on common trends), two additional explanatory variables were explored. The first focused on SWE at Lainhart Dam (Fig. 1), which has been identified as the primary managed variable in the system when developing alternate restoration scenarios for the NW Fork (SFWMD, 2006). First, SWE at Lainhart Dam was converted to flow based on the structure's rating curve. Next, a "cumulative flow deficit" (CFD) was calculated by:

$$\mathrm{CFD}(Q_{crit.})_t = \sum_{t=1}^{T} Q_{Lainhart,t} - Q_{crit.} \quad (3)$$

where $\mathrm{CFD}(Q_{crit.})$ is the cumulative flow deficit at time t (m^3), $Q_{crit.}$ is a critical daily flow rate ($m^3\ day^{-1}$), $Q_{Lainhart,t}$ is the average daily flow measured at Lainhart Dam ($m^3\ day^{-1}$). CFD accumulates daily flow "deficits" (sometimes positive, sometimes negative) over the period of record (POR), integrating changes in the volume of freshwater flow to the NW Fork over an extended period. Various DFMs were then built using $Q_{crit.}$ values of 1.0, 1.5, 1.95, 2.5, 3.0, 3.7, and 4.0 $m^3\ s^{-1}$, based on proposed restoration flows (SFWMD, 2006).

Next, since changes in SWEC appeared to be reflected in a delayed and extended manner in GWEC series, a similar transformation was applied to SWEC data. Several "cumulative salinity deviation" (CSD) series were calculated by:

$$\mathrm{CSD}_t = \sum_{t=1}^{T} \mathrm{SWEC}_t - \mathrm{SWEC}_{POR} \quad (4)$$

where CSD_t is the cumulative salinity deviation at a particular SWEC measurement location at time t (S/m), SWEC_t is the average daily surface water EC at that location at time t (S/m), and SWEC_{POR} is the average SWEC over the four-year POR (S/m). These salinity deviations were accumulated over the POR to integrate long-term changes in SWEC. The DFA was performed using CDS series calculated from SWEC series at RK 24.0, RK 14.6, RK 9.5, RK 13.1, and RK 1.1 (Fig. 1).

Please cite this article as: Kaplan, D.A., Muñoz-Carpena, R., Groundwater salinity in a floodplain forest impacted by saltwater intrusion, J. Contam. Hydrol. (2014), http://dx.doi.org/10.1016/j.jconhyd.2014.04.005

Table 3
Dynamic factor models (DFMs) tested in this study (see explanation in text).

DFM	No. of trends	Explanatory variables	Regression parameters	No. of parameters	C_{eff}
Model I	4	None	–	57	0.86
Model II	3	$R_{net,S46}$, WTE_R, $CFD_{3.0}$, $CSS_{RK9.5}$	From DFA	81	0.85
Model III	0	$R_{net,S46}$, WTE_R, $CFD_{3.0}$, $CSS_{RK9.5}$	Multiple regression	28	0.58

2.4. Analysis procedure

DFA was implemented using Brodgar software (v. 2.6.5, Highland Statistics Ltd., Newburgh, UK), which uses the statistical software language "R" (v. 2.9.1, R Development Core Team, 2009). GWEC data were converted to daily averages for use in the DFA. To compare the relative importance of common trends and explanatory variables across the set of response variables, response and explanatory variables were normalized in Brodgar (mean subtracted, divided by standard deviation) (Zuur and Pierce, 2004; Zuur et al., 2003).

The DFA was performed in three discrete steps and yielded three models (Table 3). DFMs were first developed using an increasing number of common trends until satisfactory model performance was achieved according to goodness-of-fit indicators. This DFM is referred to as Model I. Next, different combinations of explanatory variables were incorporated to reduce unexplained variability and improve description of GWEC in the floodplain. This DFM (Model II) aimed to achieve similar (or improved) goodness-of-fit metrics as Model I with fewer trends and without exceeding the VIF criterion. Finally, the best suite of explanatory variables identified in the DFA was used to create a reduced model using no common trends. This multi-linear model was created using a multiple regression code run in Matlab (2009b, The MathWorks, Inc., Natick, MA, USA) and is referred to as Model III. Removing trends from the DFM has the potential to expand model applicability (by removing reliance on unknown variation), however Model III may be limited by the ability of a linear combination of explanatory variables to reproduce non-linear interactions. For example, in a DFA of WTE in the Loxahatchee River floodplain, Kaplan et al. (2010b) found that DFMs without trends accurately predicted WTE series closer to the edges of the system where explanatory variables acted as boundary conditions, but performed worse in the interior of the system, where interactions between surface water and groundwater are most complex and nonlinear.

DFM goodness-of-fit was quantified using C_{eff} and AIC. C_{eff} compares the variance between predicted and observed data about the 1:1 line, with $C_{eff} = 1$ indicating that the plot of predicted vs. observed data matches the 1:1 line (Nash and Sutcliffe, 1970). The AIC is a statistical criterion that balances goodness-of-fit with model parsimony by rewarding goodness-of-fit but including a penalty term based on the number of model parameters (Akaike, 1974). For two different DFMs, the DFM with largest C_{eff} and smallest AIC was preferred.

3. Results and discussion

3.1. Experimental time series

3.1.1. Mean daily time series

The Loxahatchee River watershed experienced a wide range of climatic conditions over the four-year monitoring period, including four wet/dry season cycles; two very wet years with tropical storm- and hurricane-induced high water events (2004–2005); and the driest two-year period recorded in south Florida since 1932 (2006–2007; Neidrauer, 2009). Fig. 3 shows mean daily time series of selected meteorological and hydrological variables collected in the watershed over this time period. Rainfall (Fig. 3a) followed a seasonal pattern, with wet season (May–October) rain accounting for 73–80% of yearly totals over the four years (mean 77%). This is in agreement with previous seasonal rainfall observations in the Loxahatchee River Basin, which have shown that approximately two-thirds of yearly rainfall occurs in the wet season between May and October (Dent, 1997). Significant spatial variation between rainfall data collected at the S-46 and JDWX stations was observed. Though the rain gauges were only 11.2 km apart, and roughly equidistant from the shore in flat terrain, cumulative rainfall at the JDWX gauge was 2151 mm greater than that at the S-46 structure over the four-year study period, yielding divergent R_{net} series (Fig. 3b). Correlation between the rainfall time series was also low ($r^2 = 0.18$), further justifying the exploration of both series in subsequent DFM development.

Surface water elevations measured at five stations in the NW Fork are shown in Fig. 3c. Upriver SWE series (RK 23.3 and Kitching Creek) showed dynamics associated with large rainfall events and distinct dry season drawdowns. Mean daily SWE measured near T7, T8, T9, and the Jupiter Inlet were similar and overlap in Fig. 3c ($0.94 \leq r^2 \leq 0.99$ for these four series), though differences in minimum and maximum elevations were observed (see Fig. 4a–d). Common WTE trends fit to the five highest elevation wells and to nine regional groundwater wells in the Loxahatchee River (WTE_R) were similar ($r^2 = 0.75$) and mirrored the wet and dry season variations observed in the two upriver SWE series (Fig. 3d).

Calculated CFD for values of Q_{crit} ranging from 1.0 to 4.0 $m^3\ s^{-1}$ are shown in Fig. 3e and CSD series calculated from SWEC data at five locations in the NW Fork are shown in Fig. 3f. CFD time series characterize longer-term observed flow trends relative to proposed critical flows, with oscillations driven by rainfall variation between wet and dry seasons. CFD values are generally negative, reflecting dry climate conditions and/or poor water management (or both) relative to suggested ecological flow requirements (SFWMD, 2006). CSD time series characterize longer-term changes in observed surface water EC relative to average conditions. These trends are reflected in CSD declines in 2005 driven by surface water freshening from tropical storm precipitation in late 2005 and CSD increases in 2006/2007 driven by saline intrusion brought on by drought. Trends across stations are similar, but variation is highest closest to the river mouth and decreases with distance upstream.

GWEC dynamics were observed over seasonal and yearly time periods as well as over shorter time ranges

Please cite this article as: Kaplan, D.A., Muñoz-Carpena, R., Groundwater salinity in a floodplain forest impacted by saltwater intrusion, J. Contam. Hydrol. (2014), http://dx.doi.org/10.1016/j.jconhyd.2014.04.005

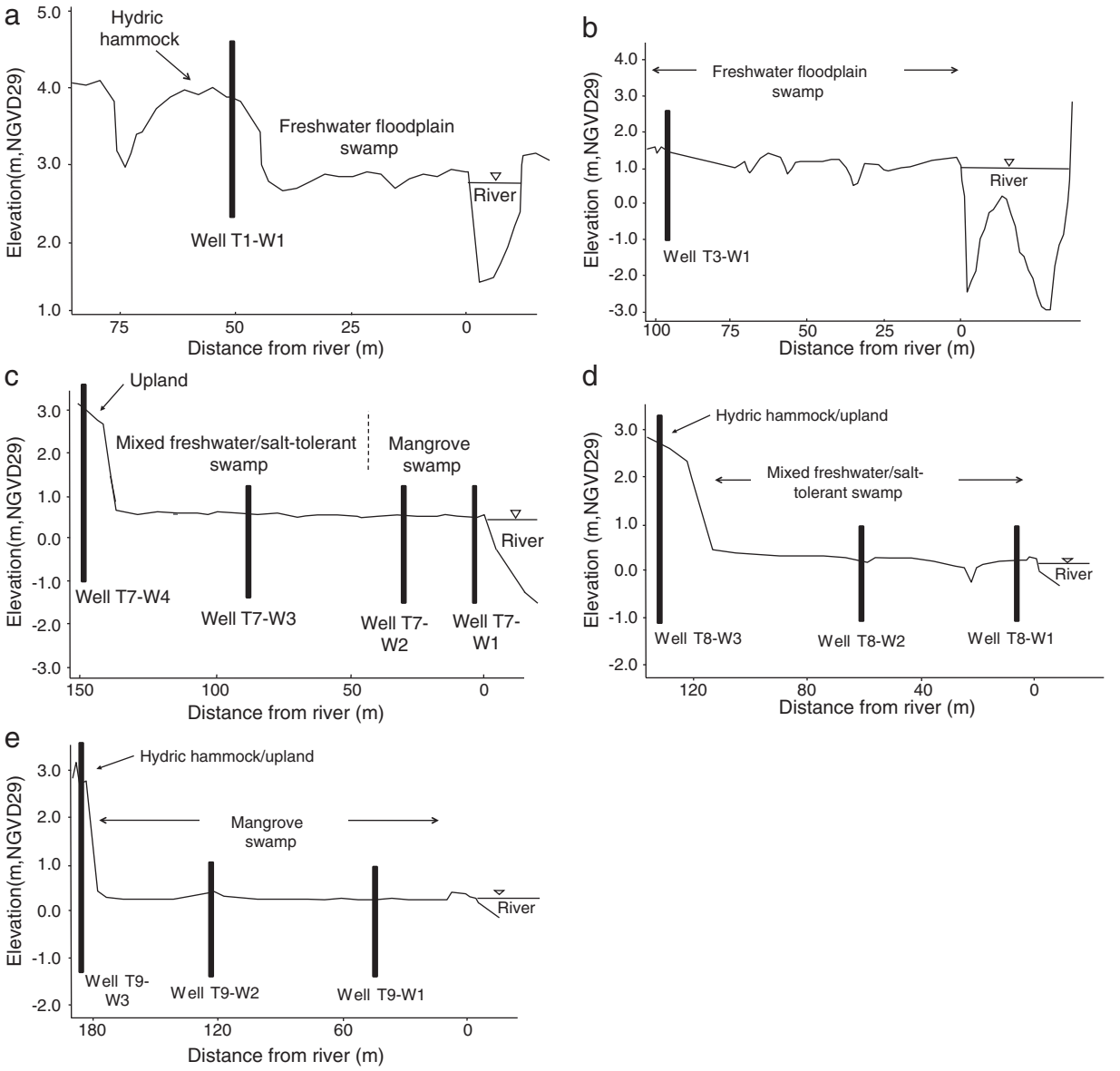

Fig. 2. Transect topographic cross-sections, detailing well installation locations and elevations and predominant vegetation cover.

(i.e., individual tidal cycles and storm events). Fig. 4 shows mean daily GWEC graphed below minimum, maximum, and mean daily SWE and 15- or 60-minute and mean daily SWEC in the adjacent river channel. These data describe the long-term surface and groundwater dynamics from upstream, riverine reaches dominated by freshwater vegetation (T1 and T3; Fig. 4a) to upper and lower tidal reaches with transitional and estuarine swamp (T7, T8, and T9; Fig. 4b–d). In general, GWEC was low in upstream and high-elevation wells and increased with proximity to the river mouth and decreasing elevation.

On upstream transects T1 and T3, GWEC remained well below a 2 ppt (0.3125 S/m) salinity tolerance threshold identified for the maintenance of a healthy bald cypress ecosystem (Liu et al., 2006) and was not a significant source or store of salts in the floodplain (Fig. 4a, lower panel). A parallel study of vadose zone hydrology (Kaplan et al., 2010a) found soil porewater EC on T1 to be higher than the GWEC observed here, likely due to concentration of solutes by evapotranspiration, though it also remained below the 0.3125 S/m threshold. Thus, vegetative changes observed in these reaches (SFWMD, 2006, 2009) may be attributed to reduced soil moisture and insufficient hydroperiod alone; it is unlikely that salinity is a contributing factor. While a strong negative correlation ($r^2 = 0.72$, $p < 0.0001$) existed between upstream SWE and SWEC, correlations between these surface water data and GWEC in wells T1-W1 and T3-W1 were low ($0.02 \leq r^2 \leq 0.14$).

On downstream transects with multiple wells, GWEC was generally highest close to the river and decreased with distance towards the upland. On T7, this trend reversed in 2007, when GWEC in well T7-W2 surpassed that of well T7-W1 and remained higher for the duration of the year before falling in

Please cite this article as: Kaplan, D.A., Muñoz-Carpena, R., Groundwater salinity in a floodplain forest impacted by saltwater intrusion, J. Contam. Hydrol. (2014), http://dx.doi.org/10.1016/j.jconhyd.2014.04.005

2008 (Fig. 4b). On T7, the 0.3125 S/m threshold was exceeded for only 3 days in 2008 (in well T7-W2) despite higher SWEC values in the adjacent river channel and daily tidal inundation of the floodplain on this transect (note different y-axes on SWEC and GWEC panels in Fig. 4b). The distinct SWEC peaks observed at RK 14.6 during the dry season were less distinct, delayed, or absent in GWEC series on the adjacent floodplain at T7. As a result, correlations between SWEC and GWEC on T7 were low ($0.02 \leq r^2 \leq 0.18$). In wells T7-W1, T7-W2, and T7-W3, GWEC returned to background levels after these SWEC peaks, indicating that salts did not accumulate in the shallow groundwater but were flushed during wet seasons. Lowest average GWEC among the twelve wells in the study was observed in well T7-W4. The fresh nature of this water and maintenance of high water table elevation in this location (Kaplan et al., 2010b) likely play a large role in maintaining the floodplain GWEC below the critical threshold on T7. The presence of salt-tolerant mangroves close to the river on this

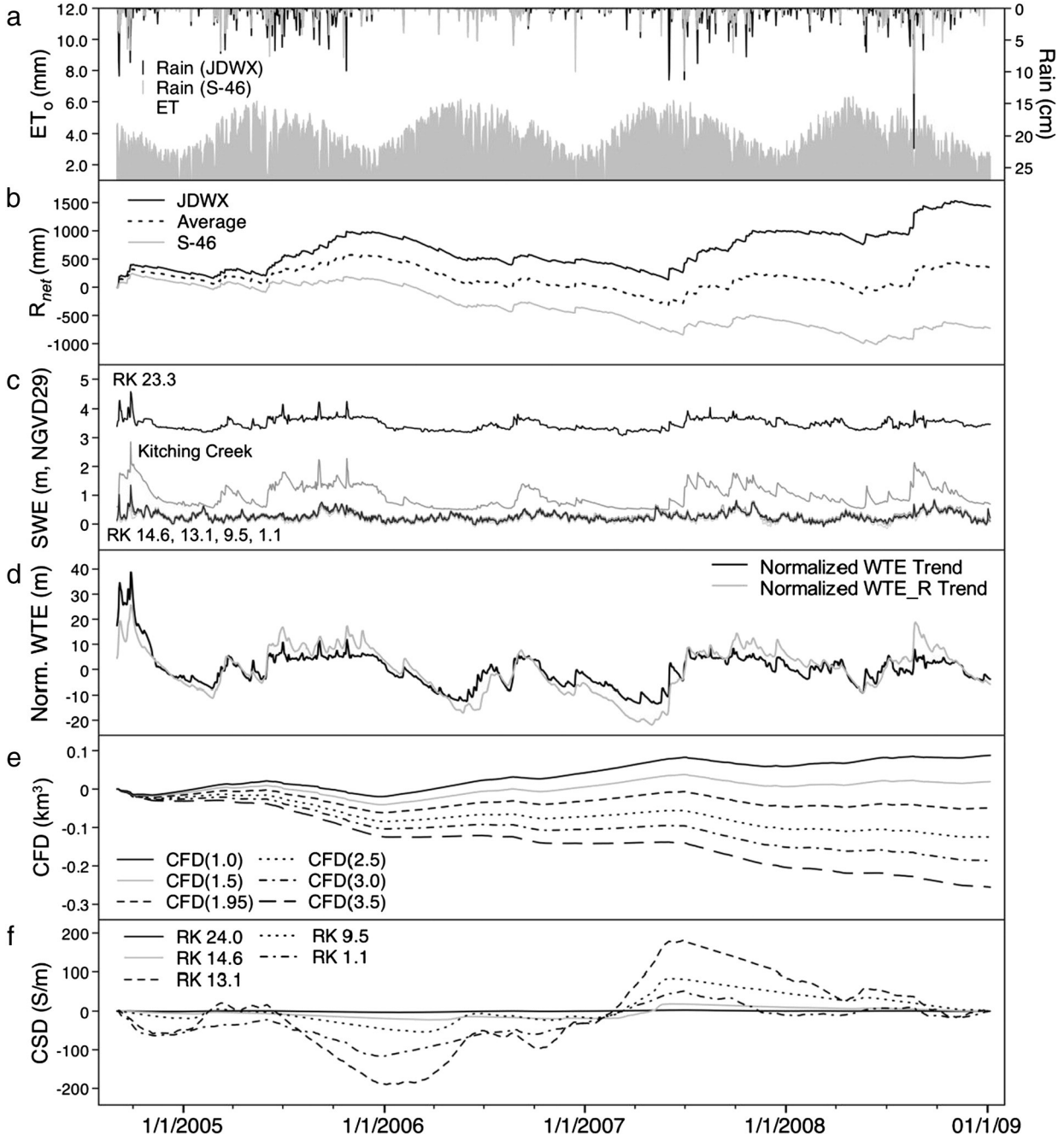

Fig. 3. Precipitation, reference evapotranspiration (ET_0), net recharge (R_{net}), surface water elevation (SWE), normalized local and regional water table elevation, cumulative flow deficit (CFD), and cumulative salinity deviation (CSD) time series measured in and around the Loxahatchee River watershed from 2004 to 2009.

Please cite this article as: Kaplan, D.A., Muñoz-Carpena, R., Groundwater salinity in a floodplain forest impacted by saltwater intrusion, J. Contam. Hydrol. (2014), http://dx.doi.org/10.1016/j.jconhyd.2014.04.005

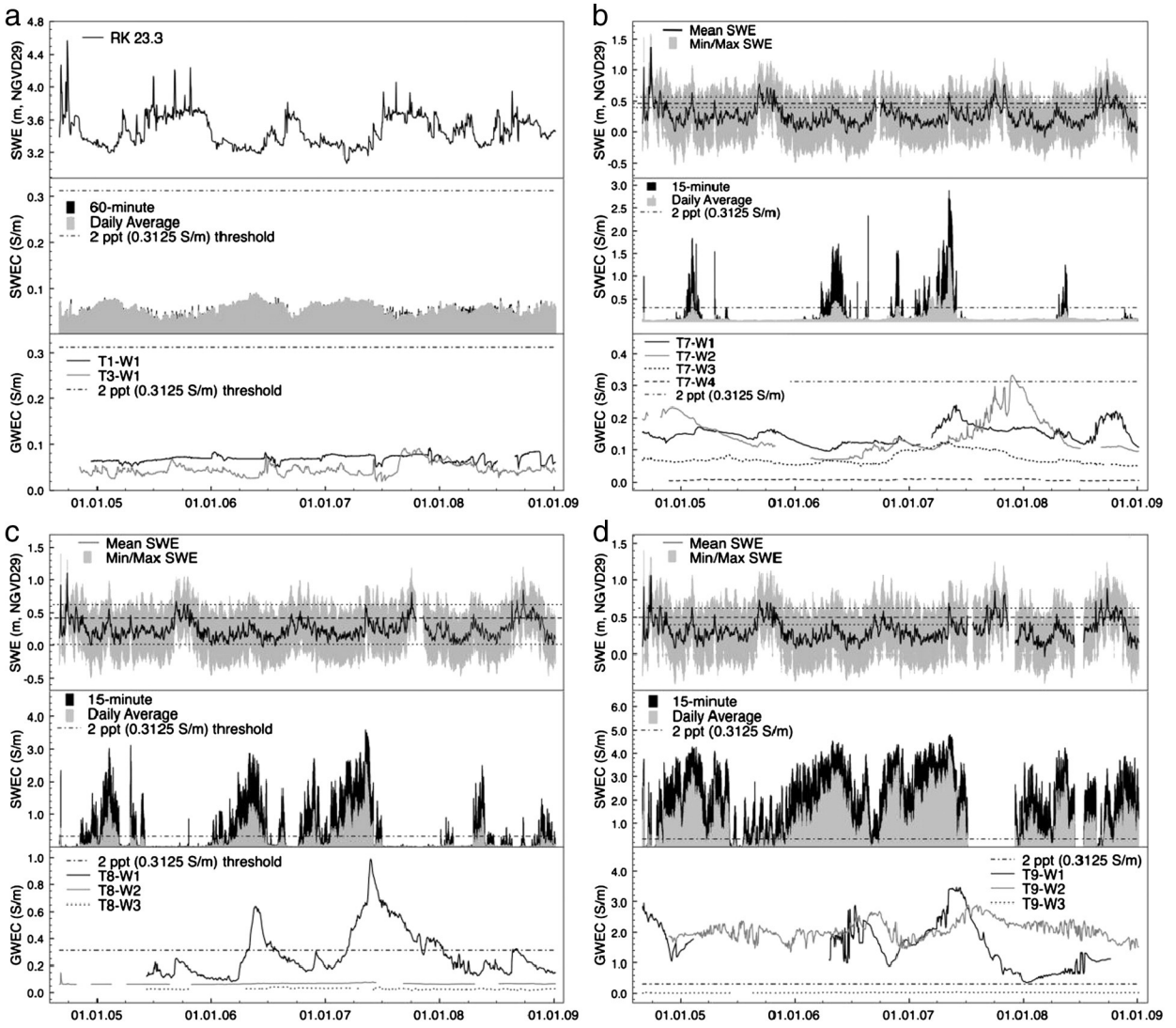

Fig. 4. Surface water elevation (SWE), surface water electrical conductivity (SWEC), and groundwater electrical conductivity on riverine transects 1 and 3 (a), upper tidal transects 7 (b) and 8 (c), and lower tidal transect 9 (d). For transects 7, 8, and 9, which receive daily tidal flooding, SWE is plotted with mean, minimum, and maximum lower floodplain elevations (dashed and dotted horizontal lines) to illustrate floodplain flooding frequency.

transect in spite of low GWEC values supports the findings of Kaplan et al. (2010a) who proposed that the distribution of freshwater and salt-tolerant plant species is driven by root zone salinity, which integrates the effects of SWEC and GWEC.

On T8, GWEC in the well closest to the river (T8-W1) was one to two orders of magnitude higher than in other wells (Fig. 4c), indicating a sharp salinity gradient in the shallow groundwater across the floodplain. This is similar to salinity patterns measured along a forest-to-marsh gradient in South Carolina (USA) by Gardner et al. (2002) and consistent with the idealized description of the saltwater wedge in the coastal aquifer (e.g., McInnis et al., 2013; Miller, 1990). GWEC in well T8-W1 surpassed the 0.3125 S/m threshold for several months in 2006 and most of 2007, but returned to background levels during wet seasons. Correspondence between peaks in GWEC in well T8-W1 and the adjacent SWEC was clearer than on T7, indicating a more direct communication between surface and groundwater in this location, though correlations between SWE and all GWEC series on T8 were still low ($0.05 \leq r^2 \leq 0.14$). GWEC in wells T8-W2 and T8-W3 remained low, except for a small increase in well T8-W2 during a tidal surge associated with Hurricane Frances in September 2004. The maintenance of low GWEC in these wells is likely due both to the maintenance of high WTE in the upland and lower floodplain inundation frequency as elevation increases with distance from the river (Fig. 2). While slightly higher elevations towards the upland currently prevent daily tidal inundation over the entire transect length, predicted sea level rise of 18 to 59 cm over the next century (IPCC, 2007) make it likely that a transition towards salt-tolerant vegetation will continue.

On lower tidal transect T9, wells T9-W1 and T9-W2 had the highest GWEC of any wells in the study, while GWEC in well T9-W3 was two orders of magnitude lower (Fig. 4d), despite

Please cite this article as: Kaplan, D.A., Muñoz-Carpena, R., Groundwater salinity in a floodplain forest impacted by saltwater intrusion, J. Contam. Hydrol. (2014), http://dx.doi.org/10.1016/j.jconhyd.2014.04.005

their similar slotted elevations (Table 1), again indicating a sharp salinity gradient. Whereas GWEC on T7 and T8 never reached the magnitude of adjacent SWEC at those transects, GWEC maxima in wells T9-W1 and T9-W2 and SWEC maxima were of similar magnitude at T9 (3–4 S/m, more than ten times the 0.3125 S threshold). Accordingly, vegetation on T9 is dominated by salt-tolerant white and red mangrove. GWEC was usually highest in well T9-W2 (Fig. 4d), though peak GWEC was observed in well T9-W1 in 2007. GWEC in well T9-W1 oscillated between high and low values over the POR, indicating some flushing of salts from the shallow groundwater, while GWEC in well T9-W2 was more constant, likely due to prolonged ponding of saline surface water behind elevated trails built on the peninsula in the 1960s (Roberts et al., 2008; Fig. 2). Again, correlations between SWEC and GWEC series were low ($0.03 \leq r^2 \leq 0.07$).

3.1.2. Thirty-minute time series

While the dynamics of mean daily GWEC variation likely provide sufficient information at the management time scale (i.e., daily to monthly), the high temporal resolution of the dataset allows us to observe additional WTE and SWEC dynamics over diurnal/tidal cycles and during storm events. For example, Fig. 5 shows the effect of tidal forcing on upper tidal transect T8 over a one-week period of high SWEC in May 2006. WTE peaks in well T8-W1 (dotted line) were coincident with tidal SWE (solid gray line), but the signal was damped in wells T8-W2 (dashed line) and T8-W3 (solid black line). During this time, the maximum tidal amplitude was 0.84 m in the surface water, and fell off quickly from 0.49 in well T8-W1 to 0.24 and 0.03 m in wells T8-W2 and T8-W3, respectively.

SWEC and GWEC peaks also varied with SWE, and an extended period of high SWEC during this 8-day period resulted in an oscillating, but steadily increasing GWEC trend driven by high SWEC (note different y-axes). The total increase in GWEC over this period was ca. 0.2 S/m, with a maximal diurnal variation of ~0.07 S/m. On the other hand, GWEC in wells T8-W2 and T8-W3 remained relatively constant at around 0.066 and 0.029 S/m, respectively, varying only within a range of ±0.0005 S/m over the same time period, which is likely inconsequential to floodplain vegetation. Thus, the impact of this extended period of high SWEC on GWEC during the dry season was generally limited to the floodplain areas closest to the river on this transect. One exception to this rule was observed during higher-than-usual SWE and WTE on T8 during the storm surge associated with Hurricane Frances (September 2004), which caused an abrupt spike in GWEC in well T8-W2 (Fig. 6). GWEC returned to background levels after ca. 1 week.

Upstream, small diurnal fluctuations in WTE and GWEC can be attributed to ET. Fig. 7 shows high-resolution SWE, WTE, and GWEC data from a three-week period in Feb/March 2006. This WTE cycling was accompanied by a concomitant, but opposite, variation in GWEC, which increased slightly during the day and decreased at night (Fig. 7, dotted line in lower panel). The scale of GWEC oscillation is smaller, with maximum ET-driven daily oscillations on the order of 0.0003 S/m (i.e., ~0.002 ppt salinity). At this scale, the sharp rise in WTE and delayed flush of salts after a rain event was also clear (Fig. 7, upper panel). Downstream, combined tidal and diurnal ET signals made it more difficult to discern the effects of ET on WTE and GWEC.

3.2. Dynamic factor analysis

3.2.1. Baseline DFA (no explanatory variables)

Different DFMs were obtained by increasing the number of common trends with the goal of achieving a maximum C_{eff} and minimum AIC. For this analysis, both diagonal and non-diagonal

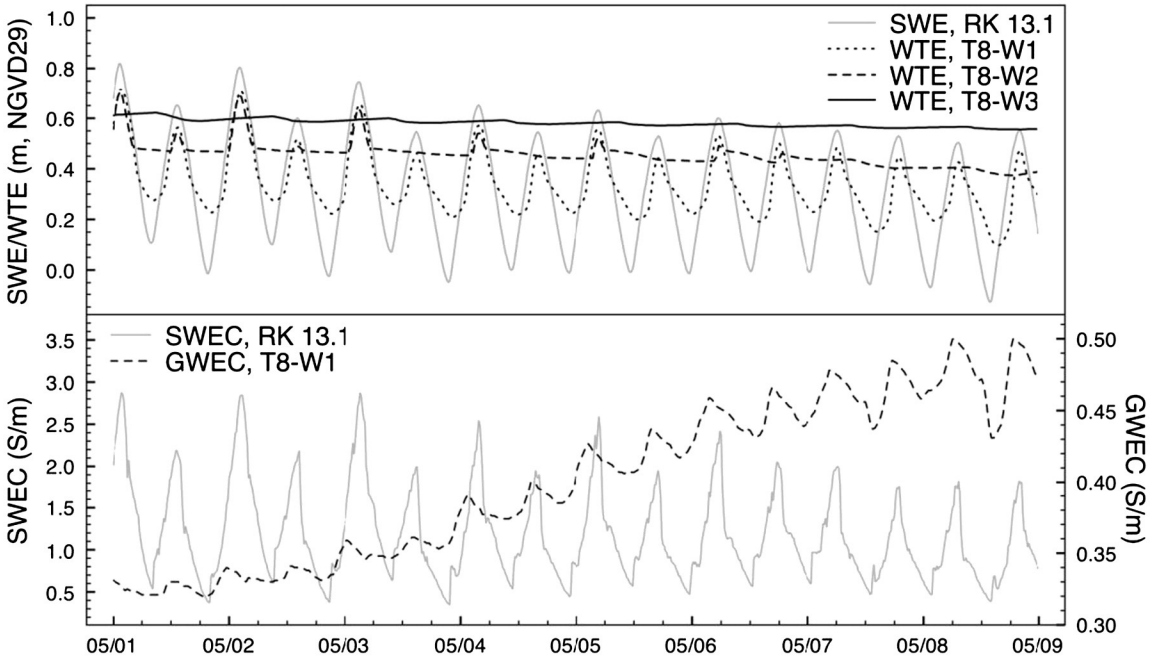

Fig. 5. High resolution (30-minute) surface water elevation (SWE), water table elevation (WTE), surface water electrical conductivity (SWEC), and groundwater electrical conductivity (GWEC) data on upper tidal transect T8 over 8 days in May 2006.

Please cite this article as: Kaplan, D.A., Muñoz-Carpena, R., Groundwater salinity in a floodplain forest impacted by saltwater intrusion, J. Contam. Hydrol. (2014), http://dx.doi.org/10.1016/j.jconhyd.2014.04.005

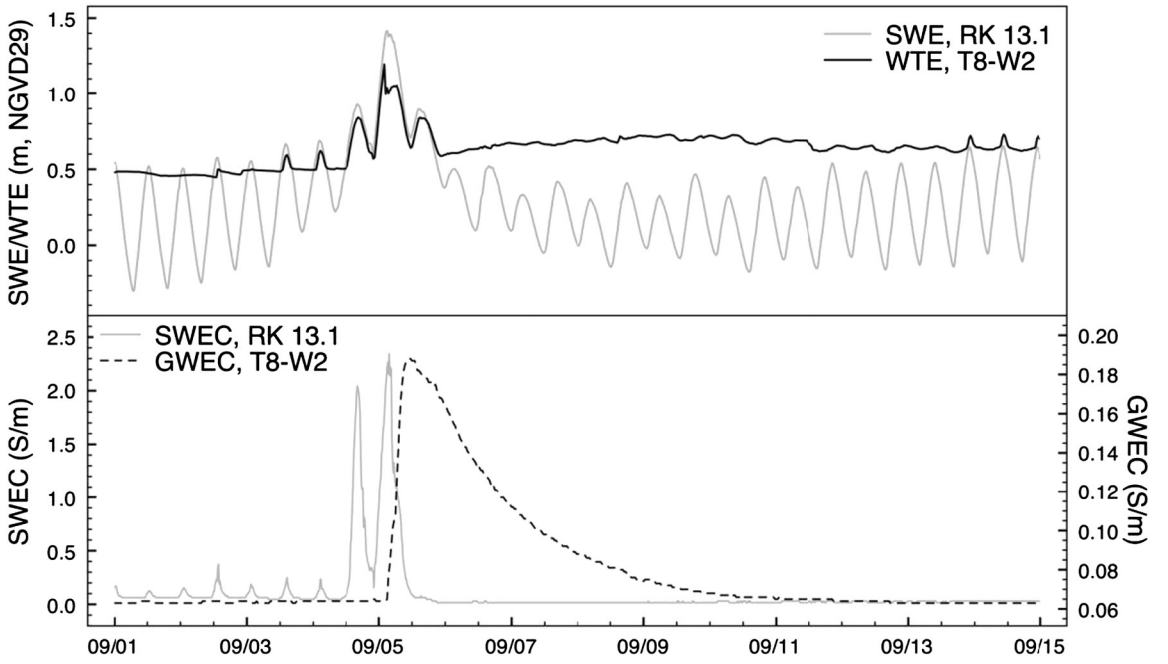

Fig. 6. High resolution (30-minute) surface water elevation (SWE), water table elevation (WTE), surface water electrical conductivity (SWEC), and groundwater electrical conductivity (GWEC) data on upper tidal transect T8 over 2 weeks in September 2004 during Hurricane Frances.

error covariance matrices were explored, however use of a diagonal matrix resulted in calculation of one or more common trends that exactly fit one or more response variables. As suggested in Highland Statistics (2000) this may occur with highly variable and noisy datasets, and a non-diagonal error matrix was used in subsequent analyses to avoid this occurrence. With a non-diagonal matrix, AIC continued to decrease and C_{eff} to increase with up to ten trends ($M = 10$). That more than ten trends (representing unexplained information) were necessary to achieve the best DFM of twelve response variables

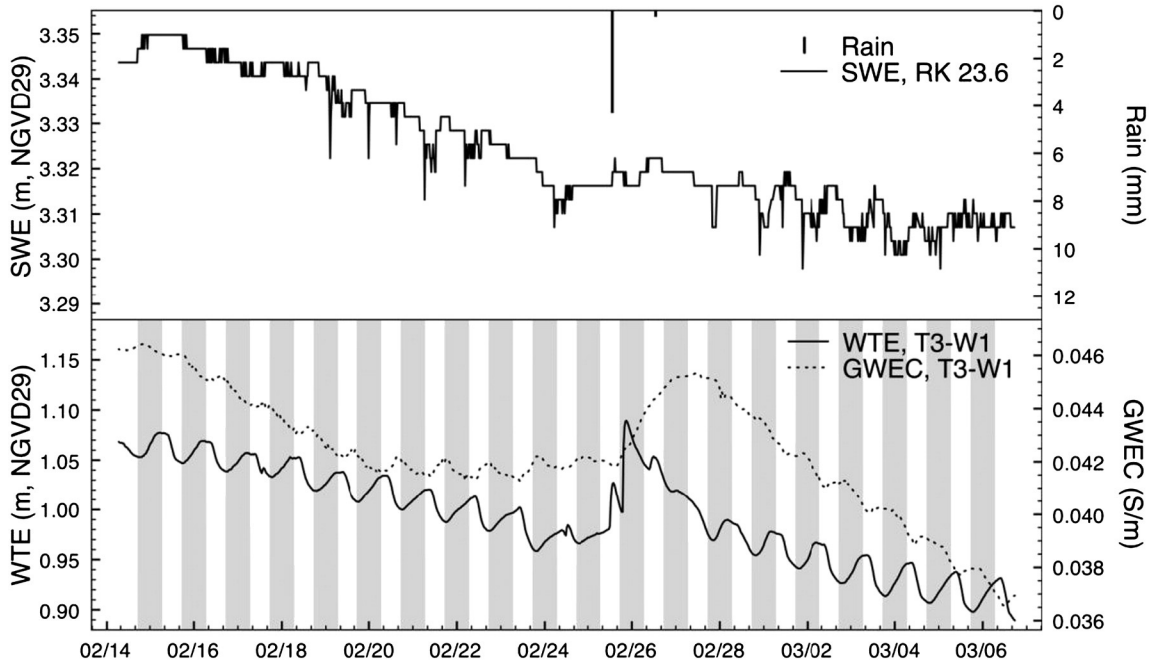

Fig. 7. High resolution (30-minute) surface water elevation (SWE), rainfall, water table elevation (WTE), and groundwater electrical conductivity (GWEC) data on upper riverine transect T3 over 3 weeks in February 2006. Gray bars indicate nighttime hours.

Please cite this article as: Kaplan, D.A., Muñoz-Carpena, R., Groundwater salinity in a floodplain forest impacted by saltwater intrusion, J. Contam. Hydrol. (2014), http://dx.doi.org/10.1016/j.jconhyd.2014.04.005

suggested that multiple latent effects influence the variability of GWEC across the watershed.

To gain more insight into possible common trends describing floodplain GWEC, a second baseline DFA was investigated with a subset of the original twelve series. Wells with low and relatively stable GWEC were excluded from this analysis. For example, GWEC in upstream and higher elevation wells T1-W1, T3-W1, T7-W4, T8-W3, and T9-W3 was never greater than 0.01 S/m (0.06 ppt). When compared with GWEC variation in the remaining seven wells, these five series may be considered as constant and of very low magnitude (Fig. 4a–d). Normalizing small variations in these series to make them useful for DFA scales up small changes, which are likely not relevant from a physical point of view. For example, these series all remained well below the 0.3125 S/m (2 ppt) bald cypress salinity tolerance threshold.

Results from the exploratory model with seven response variables ($Y = 7$; Model I) are given in Table 4. Even with the reduced set of response variables, AIC continued to decrease and C_{eff} to increase with increasing trends, with no inflection point identified. We thus balanced the incremental benefit to C_{eff} with the number of extra model parameters added with each additional trend. The added benefit to C_{eff} of additional trends tapered off after four trends (Fig. 8). Thus, for subsequent analyses and identification of explanatory variables, the baseline DFA using seven response variables ($Y = 7$) and four common trends ($M = 4$) was used. This model is referred to as Model I and had overall $C_{eff} = 0.86$ ($0.45 \leq C_{eff} \leq 0.99$) and AIC = 3463. The objective of the subsequent DFA using explanatory variables was thus to reduce the number of common trends required to achieve similar model performance to less than four in order to reduce the amount of unexplained variability in the DFM.

It is first instructive to examine the common trends from Model I and their associated canonical correlation coefficients ($\rho_{m,n}$), since high $\rho_{m,n}$ values indicate high correlation between two latent variables. The four common trends from Model I are shown in Fig. 9. Though only describing latent (unknown) variability at this stage in the DFA, these trends and their patterns of correlation are useful for developing ideas about how GWEC elevation varies in the Loxahatchee River floodplain and where to look for the most useful explanatory variables. For example, common trend 1 (Fig. 9a) was most highly correlated with GWEC in well T7-W1, but also had "moderate" correlation with well T8-W1, indicating some shared information between these two series close to the river in the upper tidal reach. Correlations with the other five wells were "low" or "minor." Common trend 2 (Fig. 5b) on the other hand was only highly correlated with GWEC in well T7-W2 and captured the extended and delayed rise in GWEC that was observed only in this location (see Fig. 4b, gray line in lower panel). All other correlations with this trend were "low" or "minor." Common trend 3 contained the most shared information, with "high" and "moderate" correlations with four of the seven wells (representing T7, T8, and T9). This trend represents the high GWEC observed in several wells in 2007. No clear spatial or physical interpretations could be drawn from common trend 4, but all correlations were "low" or "minor" for this trend, indicating a lower dependence of the DFM on this trend.

Table 4
Akaike's information criteria (AIC) and Nash–Sutcliffe coefficients of efficiency (C_{eff}) for dynamic factor models with no explanatory variables and 1–7 common trends.

M	C_{eff}	AIC
1	0.38	18,226
2	0.51	13,030
3	0.64	8489
4	0.86	3463
5	0.89	−1682
6	0.93	−6960

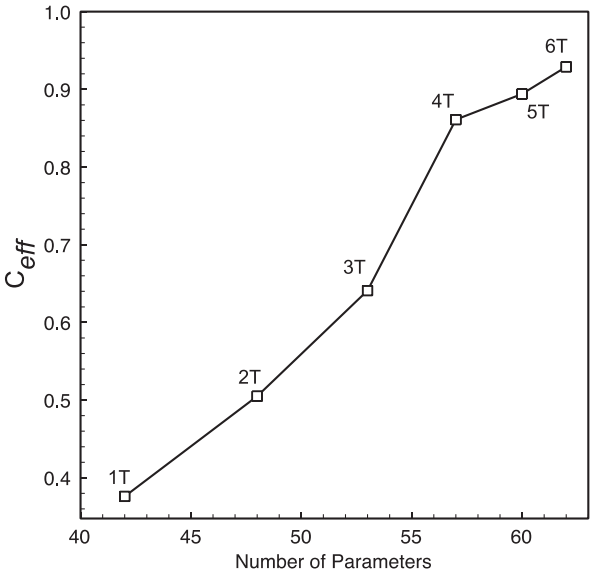

Fig. 8. Number of parameters vs. coefficient of efficiency (C_{eff}) for DFMs with one (1T) to six (6T) common trends.

3.2.2. DFA with explanatory variables

Next, appropriate explanatory variables were added to reduce the number of common trends required to achieve an adequate fit of GWEC (and to minimize the factor loadings of any remaining trends). Approximately 150 combinations of common trends and candidate explanatory variables (summarized in Table 2) were explored. Finally, the best DFM was achieved using four explanatory variables ($K = 4$): net recharge calculated with rainfall from the S46 weather station ($R_{net,S46}$), the trend representing regional groundwater circulation (WTE_R), the cumulative flow deficit with a critical flow of 3.0 $m^3\ s^{-1}$ ($CFD_{3.0}$), and cumulative salinity deviation calculated with SWEC data from RK 9.5 ($CSS_{RK9.5}$). Additional CFD and CSS series were collinear with this set of variables and were not be included in the DFM. Using both R_{net} series did not improve the model and $R_{net,S46}$ performed better than $R_{net,JDWX}$ or the average of the two series. Using these explanatory variables, it was possible to reduce the number of required common trends from four to three ($M = 3$), thus slightly reducing the unexplained variability in the model. This model (Model II) yielded AIC = 1458 and overall $C_{eff} = 0.85$ across the seven wells, improving upon the target AIC of 3463 and nearly matching the target C_{eff} of 0.86 from Model I.

Please cite this article as: Kaplan, D.A., Muñoz-Carpena, R., Groundwater salinity in a floodplain forest impacted by saltwater intrusion, J. Contam. Hydrol. (2014), http://dx.doi.org/10.1016/j.jconhyd.2014.04.005

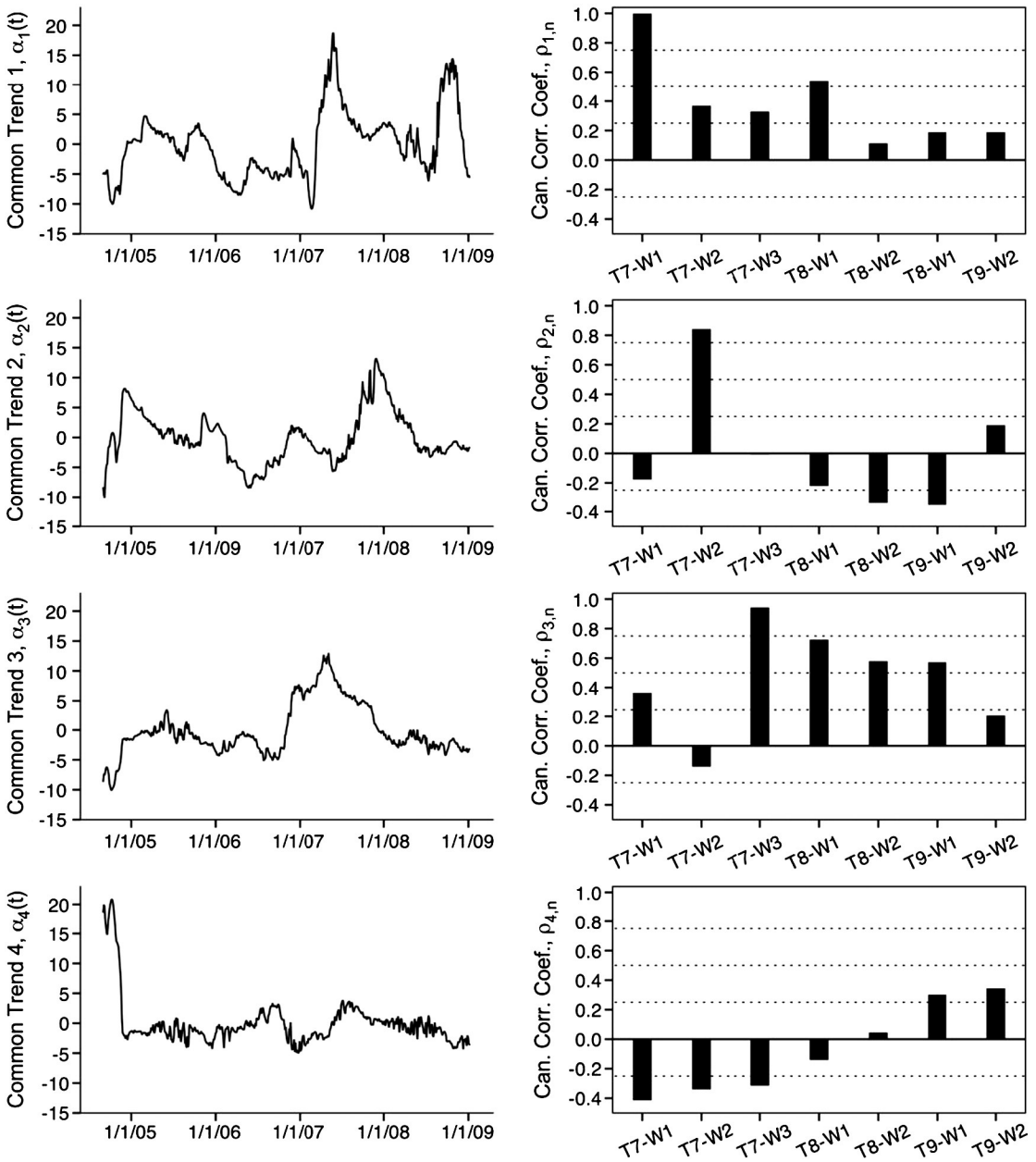

Fig. 9. Common trends (left) and their associated canonical correlation coefficients (right) for Model I.

Model II fits are illustrated in Fig. 10 and are fair to excellent ($0.52 \leq C_{eff} \leq 0.99$). Some higher elevation wells lack data from the beginning of the time series, and these model results help paint a more complete picture of GWEC in these wells during the hurricanes of 2004 (e.g., wells T8-W1 and T9-W1 in Fig. 10).

Table 5 summarizes the results obtained from Model II ($M = 3$, 4 explanatory variables). GWEC in the seven wells used in this analysis had variable relationships to the common trends, but factor loadings were reduced slightly over those in Model I. Average $|\gamma_n|$ value for the three remaining trends in Model II $= 0.07 \pm 0.06$ compared to average $|\gamma_n| = 0.10 \pm 0.11$ for the four trends in Model I. This small reduction in dependence on common trends indicated that a multilinear model without trends (Model III) might not be sufficient to describe the observed GWEC dynamics (see following section).

The $\beta_{k,n}$ in Table 5 represent the importance of a corresponding explanatory variable on each response variable in Model II, and significant regression coefficients ($\beta_{k,n}$ with t-value > 2) are shown in bold. Though variably significant to the GWEC time series, $\beta_{k,n}$ for the calculated variables CFD and CSD were more significant than any of the "raw" explanatory variables explored (e.g., SWE, SWEC, etc.). Incorporating these cumulated "memory" variables was important for improving the DFM since GWEC series varied in a delayed and extended manner compared with other hydrological variables. In addition

Please cite this article as: Kaplan, D.A., Muñoz-Carpena, R., Groundwater salinity in a floodplain forest impacted by saltwater intrusion, J. Contam. Hydrol. (2014), http://dx.doi.org/10.1016/j.jconhyd.2014.04.005

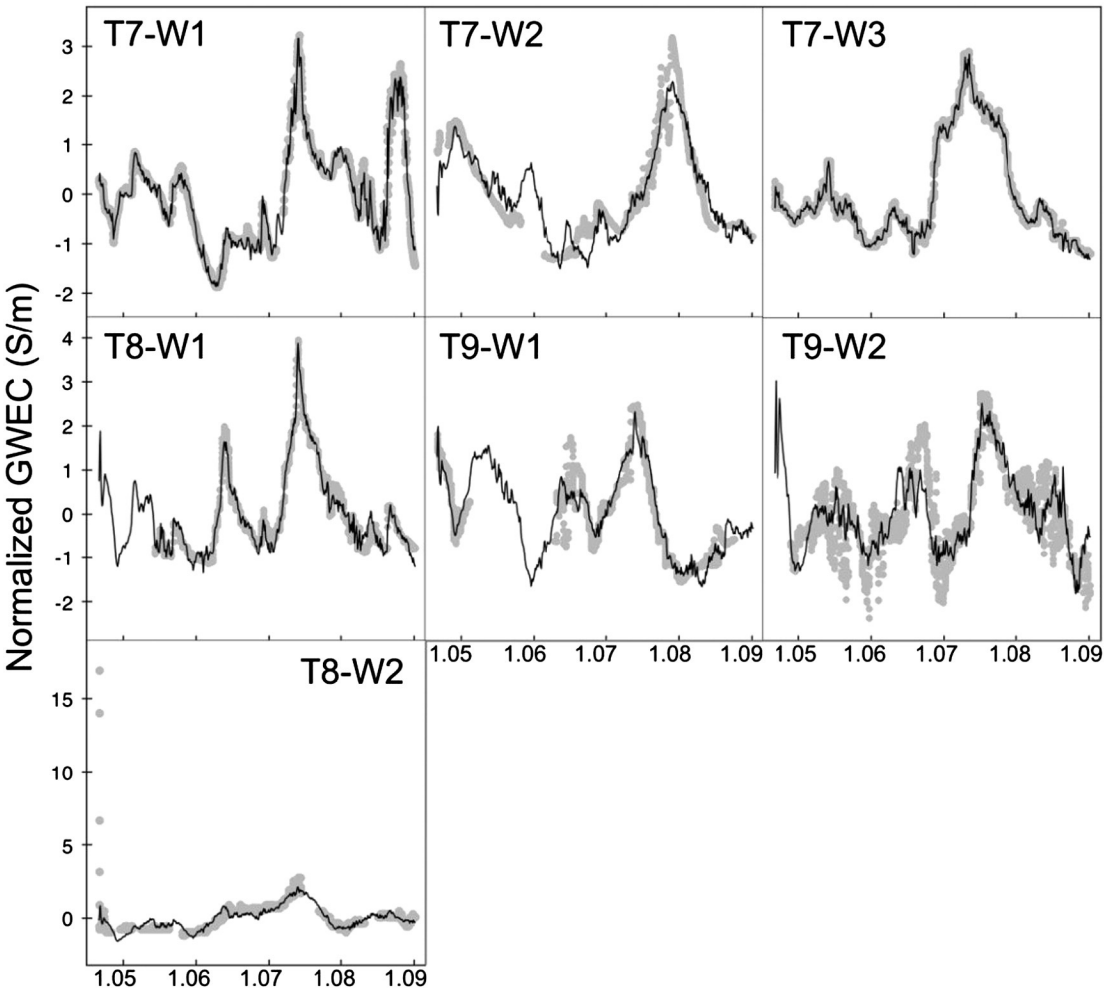

Fig. 10. Observed (gray symbols) and modeled (black lines) normalized WTE for the twelve wells obtained from Model II using 3 common trends and 5 explanatory variables.

to their statistical significance to the model, the relative importance of these environmental drivers is indicated by the magnitude of their associated $\beta_{k,n}$. Average absolute values of $\beta_{k,n}$ were 1.08, 0.75, 0.44, and 0.02 for CSD, CFD, and R_{net}, and WTE_R respectively, indicating strong correlation between calculated "memory" variables and GWEC. Despite being significant for three of the seven response variables, $\beta_{k,n}$ values for regional water table elevation were extremely low. Removing this variable from the DFM, however, yielded unsatisfactory model performance (AIC and C_{eff}) relative to Model I, so it was maintained in the DFM.

The remaining three trends in Model II and their associated $\rho_{m,n}$ values are given in Fig. 11. These trends represent the remaining unexplained (latent) variability among the GWEC

Table 5
Constant level parameters (μ_n), canonical correlation coefficients ($\rho_{m,n}$), factor loadings ($\gamma_{m,n}$), regression coefficients ($\beta_{k,n}$), and coefficients of efficiency (C_{eff}) from Model II (3 trends, 5 explanatory variables). Significant regression parameters in bold.

s_n	μ_n	Canonical correlations			Factor loadings			Regression coefficients ($\beta_{k,n}$)				$C_{eff,n}$
		$\rho_{1,n}$	$\rho_{2,n}$	$\rho_{3,n}$	$\gamma_{1,n}$	$\gamma_{2,n}$	$\gamma_{3,n}$	$R_{net,S46}$	WTE_R	$CFD_{3.0}$	$CSS_{RK9.5}$	
T7-W1	−0.49	0.73	0.05	0.01	0.19	0.00	0.01	**0.53**	0.02	−0.32	**1.49**	0.99
T7-W2	0.00	0.04	−0.41	0.17	0.02	−0.11	−0.04	**0.35**	**−0.02**	**−1.21**	**1.39**	0.88
T7-W3	0.12	0.05	0.34	0.67	0.01	0.03	0.15	0.21	0.00	0.38	0.43	0.99
T8-W1	−0.24	0.26	0.71	0.04	0.05	0.17	0.04	**−0.08**	0.01	**−1.10**	**2.14**	0.97
T8-W2	−0.03	0.05	0.46	0.17	0.01	0.12	0.09	**−0.38**	**0.02**	0.32	0.21	0.52
T9-W1	−0.07	0.27	0.70	−0.02	0.00	0.12	0.03	**0.96**	0.00	**0.93**	0.43	0.86
T9-W2	0.17	−0.29	0.52	0.02	−0.09	0.16	0.01	**−0.55**	**0.06**	−1.00	**1.47**	0.72
											Overall	0.85

Please cite this article as: Kaplan, D.A., Muñoz-Carpena, R., Groundwater salinity in a floodplain forest impacted by saltwater intrusion, J. Contam. Hydrol. (2014), http://dx.doi.org/10.1016/j.jconhyd.2014.04.005

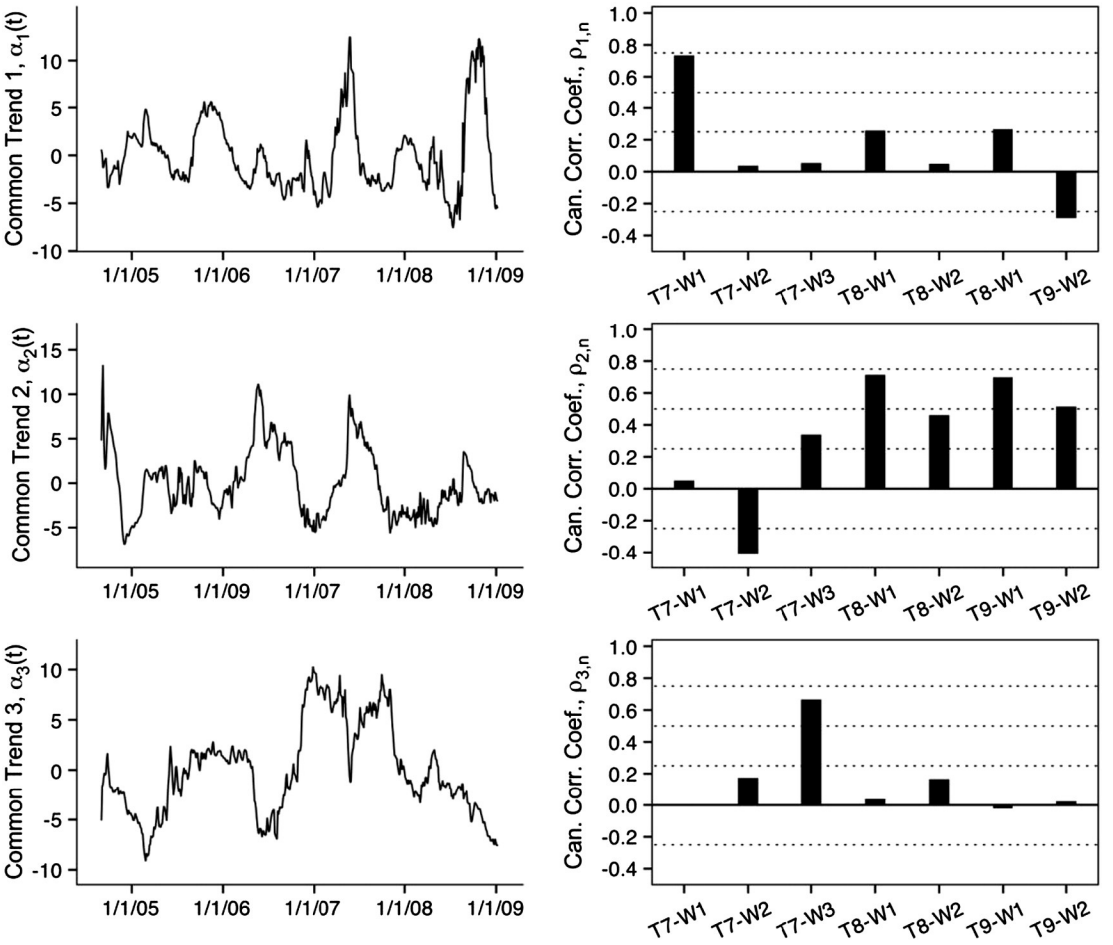

Fig. 11. Common trends (left) and their associated canonical correlation coefficients (right) for Model II.

series. The reduction in the dependence on common trends from Model I to Model II is evidenced by lower canonical correlations (e.g., no "high" correlations). Again, the relationships to trends were variable across wells. As with Model I, Trend 1 was most correlated with GWEC in well T7-W1, and described variation specific to this well. Trend 2 had "moderate" or "low" correlations with 6 of the 7 wells and the shape of the trend suggests that it captured high GWEC events in Fall 2004 (during Hurricanes Frances and Jeanne) and during the dry seasons of 2006 and 2007. Trend 3 was "moderately" correlated with GWEC in well T7-W3, but had only minor correlations with the remaining six wells.

3.2.3. Multilinear regression model (DFA with no common trends)

Finally, common trends were removed from the model to assess the validity of a DFM using only explanatory variables. In this model (Model III), the four explanatory variables identified in the DFA were used to create a multi-linear model of the response variables. As expected, C_{eff} values for Model III were reduced from Model II (overall $C_{eff} = 0.58$, $0.38 \leq C_{eff} \leq 0.75$; Table 6). Similar to $\beta_{k,n}$, model parameters in Table 6 represent the importance of explanatory variables on the response variables in Model III, with significant parameters shown in bold. With common trends removed, 26 of 28 parameters (93%) were significant to Model III, compared to 16 of 28 (57%) in Model II, suggesting that process for identifying explanatory variables in Model II is robust. The relative importance of explanatory variables in Model III mirrored that from Model II, with average absolute model parameter values of 0.81, 0.73, 0.41, and 0.03 for CSD, CFD, and R_{net}, and WTE_R, respectively. These results indicate that, in general, surface water salinity (as characterized by CSD) is the most important driver of GWEC, followed closely by freshwater flow (characterized by CFD), while R_{net} is less important and WTE_R is relatively unimportant. Critically, however, this ordering is not consistent across measurement locations, with differences in the importance of environmental variables likely driven by the specifics of well location (e.g., floodplain elevation and distance from the river mouth).

The best and worst model fits from Model III (by C_{eff}) indicate that the model without trends may adequately describe observed GWEC variation in some areas (e.g., well T7-W2, Fig. 12a), but not in others (e.g., well T9-W2, Fig. 12b). In locations where the performance of Model III is deemed adequate, it can be useful for assessment of Loxahatchee River restoration scenarios, especially considering the wide range of climatic conditions captured in the study. It is critical to note, however, that any application of Model III outside of the POR

Please cite this article as: Kaplan, D.A., Muñoz-Carpena, R., Groundwater salinity in a floodplain forest impacted by saltwater intrusion, J. Contam. Hydrol. (2014), http://dx.doi.org/10.1016/j.jconhyd.2014.04.005

Table 6
Model parameters and coefficients of efficiency (C_{eff}) from Model III (no trends, 4 explanatory variables). Significant model parameters in bold.

s_n	Model parameters				C_{eff}
	$R_{net,S46}$	WTE_R	$CFD_{3.0}$	$CSS_{RK9.5}$	
T7-W1	**0.28**	**0.02**	**0.44**	**0.43**	0.49
T7-W2	**0.07**	**0.02**	**−1.48**	**1.77**	0.75
T7-W3	**0.45**	**−0.05**	0.05	**0.88**	0.60
T8-W1	**0.46**	**−0.05**	**−0.27**	**1.13**	0.70
T8-W2	−0.05	**−0.03**	**0.50**	**−0.16**	0.43
T9-W1	**1.39**	**−0.03**	**1.68**	**−0.30**	0.73
T9-W2	**−0.15**	**0.02**	**−0.66**	**0.99**	0.38
				Overall	0.58

implicitly assumes that relationships between response and explanatory variables remain consistent, which may not be the case under non-stationary climate conditions. Moreover, while the general hydrological relationships developed in this study are likely transferrable to other systems, the statistical nature of our modeling approach limits application outside of the Loxahatchee River floodplain.

4. Summary and conclusions

The processes driving saltwater intrusion in shallow groundwater are complex, but critical to understanding and forecasting ecological change in coastal forests. This study employed a statistical modeling approach to analyze four years of high spatial and temporal resolution hydrological data collected in and around the Loxahatchee River watershed in south Florida (USA), which has been affected by reduced hydroperiod and increased saltwater intrusion. Data were modeled using dynamic factor analysis (DFA), with three primary goals: 1) to gain insight into system behavior; 2) to identify environmental variables that drive (or at a minimum are correlated with) GWEC; and 3) to yield a model that can be used (within appropriate limits) for scenario analysis, forecasting, or hindcasting.

Short- and long-term shallow groundwater electrical conductivity (GWEC) dynamics were observed in the floodplain wetlands along a salinity gradient from upstream freshwater through downstream saline river reaches. Sharp GWEC gradients were observed laterally along the floodplain, with highest GWEC observed closest to the river. Surface water electrical conductivity (SWEC) and GWEC were poorly correlated (Fig. 4); while daily SWEC maxima exceeded daily GWEC maxima in all locations, seasonal and yearly average salinities were often higher in the shallow groundwater. This phenomenon is concordance with our understanding of differences in travel and residence times in groundwater vs. surface water systems, but has implications for the ecological ramifications of pulsed salinity events on floodplain vegetation. For example, saline transgressions at T7 led to SWEC above the 0.3125 S/m threshold for 64 days in 2007 but the corresponding peak in GWEC lasted over 9 months. While GWEC only exceeded the critical threshold for 3 days, recent work (Middleton, 2009) has identified important impacts of chronic, low-level salinity on the production and regeneration potential of bald cypress, highlighting the need for a better understanding of the relationship between short-term pulses and long-term effects.

High-resolution (30-minute) GWEC data provided insights on the variety of mechanisms driving solute fluxes from surface water to groundwater (e.g., via the relatively slow, diffusive-type flux shown in Fig. 5 vs. the rapid adjective-type transport via saline water inundation shown in Fig. 6). These data also revealed daily oscillations in GWEC in both tidal (Fig. 5) and riverine reaches (Fig. 7), though they had different driving forces (tidal forcing and ET, respectively). Flushing of salts from the shallow groundwater was also observed in both upstream and downstream reaches, whether after hurricane-induced tidal inundation of saline water in the upper tidal floodplain (Fig. 6), or after a rain event in the riverine floodplain (Fig. 7, upper panel). On lower tidal transect T9, some flushing of accumulated salts occurred in well T9-W1 (Fig. 4d, black line in lower panel), but not in well T9-W2 (gray line in lower panel), likely due to several raised berms built on the peninsula, which increase infiltration of saline surface water into the shallow groundwater.

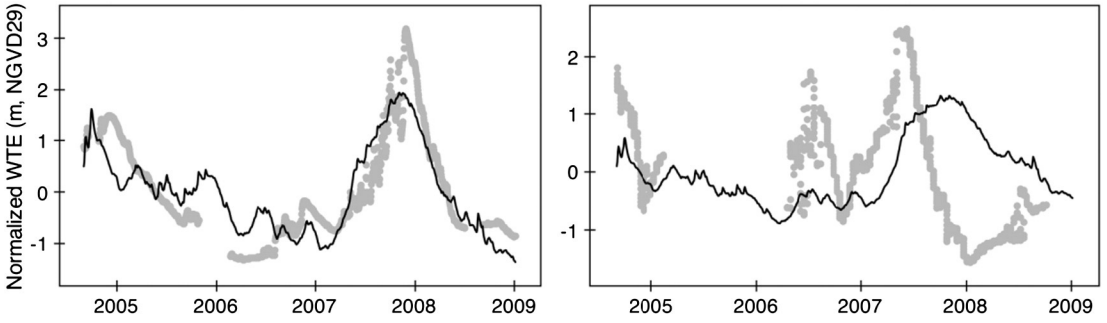

Fig. 12. Observed (gray symbols) and modeled (black lines) normalized WTE for the best and worst performing wells (T7-W2, left and T9-W2, right) obtained from Model III using 4 explanatory variables and no trends.

Please cite this article as: Kaplan, D.A., Muñoz-Carpena, R., Groundwater salinity in a floodplain forest impacted by saltwater intrusion, J. Contam. Hydrol. (2014), http://dx.doi.org/10.1016/j.jconhyd.2014.04.005

Dynamic factor analysis was performed on seven of the twelve GWEC time series that had environmentally relevant GWECs and proved to be a useful tool for the study of interactions among these response variables. A dynamic factor model (DFM) consisting of three common trends and four explanatory variables (Model II) simulated observed GWEC data well ($C_{eff} = 0.85$; $0.52 \leq C_{eff} \leq 0.99$). Model II used cumulative net recharge R_{net}, regional water table elevation (WTE_R), cumulative flow deficit (CFD), and cumulative salinity deviation (CSD) as explanatory variables. While the relative importance of these explanatory variables was specific to each response variable, CSD and CFD had the highest average model weights (regression parameters), followed by R_{net} and WTE_R.

Model II is useful for filling data gaps during the study period and for identifying the relative importance of and relationships between hydrological variables, but cannot be applied outside of the period of record (POR) due to its reliance on common trends (unknown variance), which are not predicted outside of the POR. A reduced model with no common trends (Model III) did a fair to good job (overall $C_{eff} = 0.58$, $0.38 \leq C_{eff} \leq 0.75$) simulating observed GWEC data. Despite this decease in model performance, Model III may be applied to forecast the likely impacts of management and restoration scenarios on GWEC in the Loxahatchee River floodplain. As with any statistical forecasting model, caution must be taken when applying Model III outside of the POR, since climate (and management) non-stationarity may lead to shifts in the relationships between response and explanatory variables.

Acknowledgments

This work was funded in part by the South Florida Water Management District (SFWMD) (PO4500030399). The authors would like to thank Fawen Zheng, Gordon Hu, Yongshan Wan, and Marion Hedgepeth (SFWMD) for their support and assistance interpreting groundwater data. Special thanks to Rob Rossmanith (Florida Park Service) for downloading data and maintaining field equipment under brutal field conditions. The authors also thank James Jawitz and Michael Annable for their time and effort organizing the 2013 Groundwater Quality Conference in Gainesville, FL.

References

Addis, P., Dean, J.M., Pesci, P., Locci, I., Cannas, R., Corrias, S., Cau, A., 2008. Effects of local scale perturbations in the Atlantic bluefin tuna (*Thunnus thynnus* L.) trap fishery of Sardinia (W. Mediterranean). Fish. Res. 92, 242–254.

Akaike, H., 1974. A new look at the statistical model identification. IEEE Trans. Autom. Control 19, 716–723.

Barlow, P.M., 2003. Ground water in freshwater–saltwater environments of the Atlantic coast. USGS Circular 1262. U.S. Geological Survey.

Bechtol, V., Laurian, L., 2005. Restoring straightened rivers for sustainable flood mitigation. Disaster Prev. Manag. 14, 6–19.

Burkett, V., Codignotto, J.O., Forbes, D.L., Mimura, N., Beamish, R.J., Ittekkot, V., 2001. Coastal zones and marine ecosystems. In: McCarthy, J., Canziani, O., Leary, N., Dokken, D., White, K. (Eds.), Climate Change 2001:Impacts, Adaptation & Vulnerability, Contribution of Working Group II to the Third Assessment Report of the Inter-governmental Panel on Climate Change (IPCC). Cambridge University Press, New York.

Campo-Bescos, M., Muñoz-Carpena, R., Kaplan, D., Southworth, J., Zhu, L., Waylen, P., 2013. Beyond precipitation: physiographic thresholds dictate the relative importance of environmental drivers on savanna vegetation. PLoS One 8 (8), e72348. http://dx.doi.org/10.1371/pone.0072348.

DeLaune, R.D., Nyman, J.A., Patrick Jr., W.H., 1994. Peat collapse, ponding and wetland loss in a rapidly submerging coastal marsh. J. Coastal Res. 10, 1021–1030.

Dempster, A.P., Laird, N.M., Rubin, D.B., 1977. Maximum likelihood from incomplete data via the EM algorithm. J. R. Stat. Soc. Ser. B 39, 1–38.

Dent, R.C., 1997. Rainfall Observations in the Loxahatchee River Watershed. Loxahatchee River District, Jupiter, Florida.

Erzini, K., 2005. Trends in NE Atlantic landings (southern Portugal): identifying the relative importance of fisheries and environmental variables. Fish. Oceanogr. 14, 195–209.

Essink, G.H.P.O., 2001. Saltwater intrusion in 3D large scale aquifers: a Dutch case. Phys. Chem. Earth 26 (4), 337–344.

Flynn, K.M., McKee, K.L., Mendelssohn, I.A., 1995. Recovery of freshwater marsh vegetation after a saltwater intrusion event. Oecologia 103, 63–72.

Gardner, L.R., Reeves, H.W., Thibodeau, P.M., 2002. Groundwater dynamics along forest–marsh transects in a southeastern salt marsh, USA: description, interpretation and challenges for numerical modeling. Wetl. Ecol. Manag. 10, 145–159.

Geweke, J.F., 1977. The dynamic factor analysis of economic time series models. p. 365–382. In: Aigner, D.J., Goldberger, A.S. (Eds.), Latent Variables in Socio-economic Models. North-Holland, Amsterdam, pp. 365–382.

Guo, W., Langevin, C.D., 2002. User's guide to SEAWAT: a computer program for simulation of three-dimensional variable density ground-water flow. US Geological Survey Open-File Report 01-434 (79 pp.).

Harvey, A.C., 1989. Forecasting, Structural Time Series Models and the Kalman Filter. Cambridge University Press, New York.

Highland Statistics, Inc., 2000. Software Package for Multivariate Analysis and Multivariate Time Series Analysis. Highland Statistics Ltd., Newburgh, UK.

IPCC, 2007. Summary for Policymakers. In: Solomon, S., Qin, D., Manning, M., Chen, Z., Marquis, M., Averyt, K.B., Tignor, M., Miller, H.L. (Eds.), Climate Change 2007: The Physical Science Basis. Contribution of Working Group I to the Fourth Assessment Report of the Intergovernmental Panel on Climate Change. Cambridge University Press, Cambridge, United Kingdom and New York, NY, USA.

Jassby, A.D., Kimmerer, W.J., Monismith, S.G., Armor, C., Cloern, J.E., Powell, T. M., Schubel, J.R., Vendlinski, T.J., 1995. Isohaline position as a habitat indicator for estuarine populations. Ecol. Appl. 5, 272–289.

Kaplan, D., Muñoz-Carpena, R., 2011. Complementary effects of surface water and groundwater on soil moisture dynamics in a degraded coastal floodplain forest. J. Hydrol. 398 (3–4), 221–234. http://dx.doi.org/10.1016/j.jhydrol.2010.12.019.

Kaplan, D., Muñoz-Carpena, R., Wan, Y., Hedgepeth, M., Zheng, F., Roberts, R., Rossmanith, R., 2010a. Linking river, floodplain, and vadose zone hydrology to improve restoration of a coastal river impacted by saltwater intrusion. J. Environ. Qual. 39 (5), 1570–1584. http://dx.doi.org/10.2134/jeq2009.0375.

Kaplan, D., Muñoz-Carpena, R., Ritter, A., 2010b. Untangling complex shallow groundwater dynamics in the floodplain wetlands of a southeastern U.S. coastal river. Water Resour. Res. 46, W08528. http://dx.doi.org/10.1029/2009WR009038.

Kovács, J., Márkus, L., Halupka, G., 2004. Dynamic factor analysis for quantifying aquifer vulnerability. Acta Geol. Hung. 47, 1–17.

Kuo, Y., Chang, F., 2010. Dynamic factor analysis for estimating ground water arsenic trends. J. Environ. Qual. 39, 176–184. http://dx.doi.org/10.2134/jeq2009.0098.

Kuo, Y., Chu, H., Pan, T., Yu, H., 2011. Investigating: common trends of annual maximum rainfalls during heavy rainfall events in southern Taiwan. J. Hydrol. 409. http://dx.doi.org/10.1016/j.jhydrol.2011.09.015.

Langevin, C., Swain, E., Wolfert, M., 2005. Simulation of integrated surfacewater/ground-water flow and salinity for a coastal wetland and adjacent estuary. J. Hydrol. 314, 212–234.

Lin, Jin, Blake Snodsmith, J., Zheng, Chunmiao, Wu, Jianfeng, 2008. A modeling study of seawater intrusion in Alabama Gulf Coast, USA. Environ. Geol. 57 (1), 119–130. http://dx.doi.org/10.1007/s00254-008-1288-y (3).

Liu, W., Hsu, M., Kuo, A.Y., Li, M., 2001. Influence of bathymetric changes on hydrodynamics and salt intrusion in estuarine system. J. Am. Water Resour. 37, 1405–1419.

Liu, G., Li, Y., Muñoz-Carpena, R., Hedgepeth, M., Wan, Y., 2006. Effects of Salinity and Flooding on Growth of Bald Cypress (Taxodium distichum (L.) Rich.). Abstracts, Intl. Ann. Joint Meet., Am. Soc. Agron., Crop Sci. Soc Am., and Soil Sci. Soc. Am., Indianapolis, IN 12–16.

Lütkepohl, H., 1991. Introduction to Multiple Time Series Analysis. Springer-Verlag, Berlin.

Lyons, M.N., Halse, S.A., Gibson, N., Cale, D.J., Lane, J.A.K., Walker, C.D., Mickle, D.A., Froend, R.H., 2007. Monitoring wetlands in a salinizing landscape: case studies from the wheatbelt region of Western Australia. Hydrobiologia 591, 147–164.

Márkus, L., Berke, O., Kovács, J., Urfer, W., 1999. Spatial prediction of the intensity of latent effects governing hydrogeological phenomena. Environmetrics 10 (5), 633–654.

McCarthy, J.J., Canziani, O.F., Neary, N.A., Dokken, D.J., White, K.S. (Eds.), 2001. Climate Change 2001: Impacts, Adaptation, and Vulnerability. Contribution of working group II to the third assessment of the Intergovernmental Panel on Climate Change. Cambridge Univ. Press, New York.

McInnis, D., Silliman, S., Boukari, M., Yalo, N., Orou-Pete, S., Fertenbaugh, C., Fayomi, H., 2013. Combined application of electrical resistivity and shallow groundwater sampling to assess salinity in a shallow coastal aquifer in Benin, West Africa. J. Hydrol. 505, 335–345.

Melloul, A., Goldenberg, L., 1997. Monitoring of seawater intrusion in coastal aquifers: basics and local concerns. J. Environ. Manag. 51, 73–86.

Middleton, B.A., 2009. Regeneration potential of baldcypress (*Taxodium distichum*) swamps and climate change. Plant Ecol. 202, 257–274.

Miller, J.A., 1990. Ground water atlas of the United States—Alabama, Florida, Georgia, and South Carolina. U.S. Geological Survey Hydrologic Atlas 730-GUSGS, Washington, DC (28 pp.).

Moffett, K.B., Tyler, S.W., Torgersen, T., Menon, M., Selker, J.S., Gorelick, S.M., 2008. Processes controlling the thermal regime of saltmarsh channel beds. Environ. Sci. Technol. 42, 671–676.

Mortl, A., Muñoz-Carpena, R., Kaplan, D., 2011. Calibration of a combined dielectric probe for soil moisture and porewater salinity measurement in three southeastern (USA) coastal floodplain soils. Geoderma 161 (1–2), 50–62. http://dx.doi.org/10.1016/j.geoderma.2010.12.007.

Motz, L.H., Sedighi, A., 2009. Representing the coastal boundary condition in regional groundwater flow models. J. Hydrol. Eng. 14, 821–831.

Muñoz-Carpena, R., Ritter, A., Li, Y.C., 2005. Dynamic factor analysis of groundwater quality trends in an agricultural area adjacent to Everglades National Park. J. Contam. Hydrol. 80, 49–70.

Muñoz-Carpena, R., Kaplan, D., Gonzalez, F.J., 2008. Groundwater data processing and analysis for the Loxahatchee River Basin. Final Project Report to the South Florida Water Management District-Coastal Ecosystems Division, SFWMD Identifier: 4500020860. August 2008. University of Florida, Gainesville.

Nash, J.E., Sutcliffe, J.V., 1970. River flow forecasting through conceptual models. Part 1—a discussion of principles. J. Hydrol. 10, 282–290.

Nassar, M.K.K., El-Damak, R.M., Ghanem, A.H.M., 2007. Impact of desalination plants brine injection wells on coastal aquifers. Environ. Geol. 54, 445–454.

Neidrauer, C., 2009. Water Conditions Summary. Florida Water Management District, Operations Control Dept., West Palm Beach, FL (Available at http://www.sfwmd.gov/portal/page/portal/pg_grp_sfwmd_governingboard/portlet_gb_subtab_presentations_page/tab20092120/3%20%20water%20conditions.pdf (verified 21 September 09)).

Ritter, A., Muñoz-Carpena, R., 2006. Dynamic factor modeling of ground and surface water levels in an agricultural area adjacent to Everglades National Park. J. Hydrol. 317, 340–354.

Ritter, A., Muñoz-Carpena, R., Bosch, D.D., Schaffer, B., Potter, T.L., 2007. Agricultural land use and hydrology affect variability of shallow groundwater nitrate concentration in South Florida. Hydrol. Process. 21, 2464–2473.

Ritter, A., Regalado, C.M., Muñoz-Carpena, R., 2009. Temporal common trends of topsoil water dynamics in a humid subtropical forest watershed. Vadose Zone J. 8 (2), 437–449.

Roberts, R.E., Hedgepeth, M.Y., Alexander, T.R., 2008. Vegetational responses to saltwater intrusion along the Northwest Fork of the Loxahatchee River within Jonathan Dickinson State Park. Florida Sci. 71, 383–397.

R Development Core Team, 2009. The R project for statistical computing, v. 2.9.1. R Foundation for Statistical Computing, Vienna, Austria http://www.Rproject.org/.

SFWMD, 2002. Technical Criteria to Support Development of Minimum Flow and Levels for the Loxahatchee River and Estuary. Water Supply Department, Water Resources Management, South Florida Water Management District, West Palm Beach, Florida (November 2002 final draft).

SFWMD, 2006. Evaluation of Restoration Alternatives for the Norwest Fork of the Loxahatchee River. Water Supply Department, Water Resources Management, South Florida Water Management District, West Palm Beach, Florida.

SFWMD, 2009. Riverine and Tidal Floodplain Vegetation of the Loxahatchee River and Its Major Tributaries. South Florida Water Management District (Coastal Ecosystems Division) and Florida Park Service (5th District), West Palm Beach, FL.

Shumway, R.H., Stoffer, D.S., 1982. An approach to time series smoothing and forecasting using the EM algorithm. J. Time Ser. Anal. 3, 253–264.

Skalbeck, John D., Reed, Donald M., Hunt, Randall J., Lambert, Jamie D., 2008. Relating groundwater to seasonal wetlands in southeastern Wisconsin, USA. Hydrogeol. J. (8). http://dx.doi.org/10.1007/s10040-008-0345-7.

Tulp, Ingrid, Bolle, Loes J., Rijnsdorp, Adriaan D., 2008. Signals from the shallows: in search of common patterns in long-term trends in Dutch estuarine and coastal fish. J. Sea Res. 60 (1–2), 54–73.

U.S. Geological Survey (USGS), 2001. Sea-level and Climate. USGS Fact Sheet 002-00. http://pubs.usgs.gov/fs/fs2-00/.

VanArman, J., Graves, G.A., Fike, D.L., 2005. Loxahatchee watershed conceptual ecological model. Wetlands 25, 926–942.

Wang, F.C., 1988. Dynamics of saltwater intrusion in coastal channels. J. Geophys. Res. 93, 6937–6946.

Wanless, H.R., 1989. The inundation of our coastlines. Sea Frontiers 35, 264–271.

Wanless, H.R., Parkinson, R.W., Tedesco, L.P., 1994. Sea level control on stability of Everglades wetlands. In: Davis, S.M., Ogden, J.C. (Eds.), Everglades: The Ecosystem and Its Restoration: Delray Beach. St. Lucie Press, Florida, pp. 199–224.

Werner, A.D., Bakker, M., Post, V.E., Vandenbohede, A., Lu, C., Ataie-Ashtiani, B., Barry, D.A., 2013. Seawater intrusion processes, investigation and management: recent advances and future challenges. Adv. Water Resour. 51, 3–26.

Wu, L.S.-Y., Pai, J.S., Hosking, J.R.M., 1996. An algorithm for estimating parameters of state-space models. Stat. Probab. Lett. 28, 99–106.

Zuur, A.F., Pierce, G.J., 2004. Common trends in Northeast Atlantic squid time series. J. Sea Res. 52, 57–72.

Zuur, A.F., Fryer, R.J., Jolliffe, I.T., Dekker, R., Beukema, J.J., 2003. Estimating common trends in multivariate time series using dynamic factor analysis. Environmetrics 14, 665–685.

Zuur, A.F., Ieno, E.N., Smith, G.M., 2007. Analysing Ecological Data. Springer.

Please cite this article as: Kaplan, D.A., Muñoz-Carpena, R., Groundwater salinity in a floodplain forest impacted by saltwater intrusion, J. Contam. Hydrol. (2014), http://dx.doi.org/10.1016/j.jconhyd.2014.04.005